ICARUS 21, 317–368 (1974)

Variable Features on Mars III: Comparison of Mariner 1969 and Mariner 1971 Photography

J. VEVERKA AND CARL SAGAN

Laboratory for Planetary Studies, Cornell University, Ithaca, New York 14850

AND

LYNN QUAM, R. TUCKER, AND B. EROSS

Artificial Intelligence Laboratory, Stanford University, Stanford, California 94305

Received October 1, 1973; revised November 12, 1973

Mariner 9 (M9) and Mariner 6 and 7 photography of common regions of Mars are compared, with appropriate attention to the photometric properties of the camera systems. The comparison provides a 2.5yr time baseline for study of variable albedo features. We find the development of bright streaks and patches, a phenomenon unobserved through the entire M9 mission; the evolution of dark crater splotches into dark streaks; and a planetwide increase in splotchiness. Yet, a large number of splotches and albedo boundaries remain fixed over the same period. Many of the observations are interpreted in terms of a global fallout and subsequent local redistribution of bright fine particulates raised by global dust storms.

Mariner 9 discovered that many classical dark markings on Mars appear to be made of dark streaks and splotches, and there is some evidence that many of the seasonal and secular changes in the dark markings are in turn due to changes in constituent streaks and splotches—changes produced by windblown sand and dust (Sagan *et al.*, 1972; Sagan *et al.*, 1973). The classical literature on variable Martian surface features (see e.g., Antoniadi, 1930; Slipher, 1962) indicates that seasonal changes evolve over major fractions of a Martian year; in addition there are secular changes which frequently require years to develop. The relatively short duration of the Mariner 9 mission (less than half a Martian year) limits the applicability of Mariner 9 data to general discussions of seasonal and secular changes on Mars. However, some information on a $2\frac{1}{2}$yr time baseline can be obtained by comparing photographs obtained by Mariners 6 and 7 in late Earth summer, 1969 with images obtained by Mariner 9 in early 1972. From their arrival times at Mars, we will call these two sets of missions Mariner '69 and Mariner '71 respectively. The areocentric longitude of the Sun, L_s, is a convenient designator of Martian season, with $L_s = 0°$ at the beginning of northern spring.

The M 69 close-encounter pictures were obtained between July 30 and August 4, 1969, or at $L_s \simeq 200°$. Thus, M 69 near-encounter photography provides a glimpse of the southern hemisphere of Mars during its early spring, a season not observed by M 71.

Most M 71 photography covers L_s values from about 321°–360° (Orbits 100 to 240); that is, late summer in the south. M 71 photography before orbit 100 is heavily obscured by atmospheric dust, and even so the range of L_s is extended to only $L_s \simeq 290°$. The few extended mission photographs provide glimpses of Mars at $L_s \simeq 40$–50°, 70°, and 100°. Therefore, in the search for seasonal changes a M 69/M 71 comparison provides areocentric longitudes and a time baseline not available from M 71 alone.

Copyright © 1974 by Academic Press, Inc.
All rights of reproduction in any form reserved.
Printed in Great Britain

In view of the different quality of the M 69 and M 71 pictures, due to different camera characteristics as well as to the different conditions under which the two sets of pictures were taken, an immediate comparison is difficult. Generally, if one looks at prints of an overlapping pair of M 69 and M 71 picture, the scales and projections are quite different, and the processing of the two pictures is not at all comparable. We have therefore chosen to carry out this study using the image differencing system developed at the Stanford Artificial Intelligence Laboratory to process Mariner '71 photography (Sagan *et al.*, 1972, 1973; Levinthal *et al.*, 1973). The M 69 picture data are read in and converted to a M 71 format; thereafter the images can be treated as M 71 pictures for picture comparison and differencing. Appropriate first-order photometric corrections are applied to both M 69 and M 71 data.

This procedure is very successful in dealing with Mariner 6 photography. It is difficult to distinguish between Mariner 6 and Mariner 9 frames when similarly processed (cf. Fig. 24 below). Unfortunately this is not the case for Mariner 7 A-frames—which always remain bland and noisy compared to Mariner 6 and 9 images of similar locales. We believe that Mariner 6 and 9 A-frames can be compared meaningfully, but the comparison with Mariner 7 photography is dubious, due to the unusual performance of the A-camera on that spacecraft.

We stress that it is not possible to compare *absolute* photometry among M6, M7, and M9. Our study is based on comparisons of *relative* photometry within single A-frames. For example, consider two nearby albedo features X and Y, whose apparent brightness (in arbitrary, but comparable units) we denote by $b(X)$ and $b(Y)$ in M6 photography and by $B(X)$ and $B(Y)$ in M9 photography. Lacking accurate absolute photometry we cannot attach any importance to findings such as: $b(X) > B(X)$ or $b(Y) < B(Y)$. We must rely on relative photometry within a single frame, and work with contrast ratios. Thus $b(X)/b(Y) < B(X)/B(Y)$ would be considered a meaningful change.

In the following study we have carried out an extensive comparison of all suitable Mariner 6 and 7 near-encounter pictures with corresponding Mariner 9 frames. Mariner 7 frames of the south polar cap are not included.

In our analysis we have generally chosen scales which use the full resolution of the M6 and M7 imagery, and which consequently degrade somewhat the resolution available in M9 A-frames. Two types of products were often generated:

1. "*contrast stretched*," in which the scene contrast is linearly enhanced; and
2. "*high-pass filtered and contrast stretched*," in which a two-dimensional high pass filter is applied to the picture data to remove low spatial frequency changes in brightness before the contrast is linearly enhanced.

These two processes are described by Levinthal *et al.* (1973).

For each picture difference the figure caption gives the scale factor K in km/pixel corresponding to the pixel scales shown. On these scales the smallest division represents 5 pixels.

The paper is divided into four major parts. In Parts I and II we given a detailed account of our study of, respectively, Mariner 6 and 7 low-resolution, A-camera frames. Part III contains the details of the study of B-camera frames; Part IV comprises a summary of the findings and a discussion of their implications.

I: Mariner 6 A-Frames

Of the Mariner 6 near-encounter A-frames, 6N1, 6N3, 6N5, and 6N7 are severely foreshortened, making a meaningful comparison with Mariner 9 data impossible. 6N9 and 6N17 cannot be used since they are taken through a blue filter, and cannot be expected to show albedo markings well. Of the remaining six A-frames, four (6N11, 6N15, 6N19, and 6N23) are taken with a green filter; two (6N13, 6N21) are taken with the red filter. Part of 6N23 overlaps 6N21; the remainder is very close to the terminator, and is not suitable for our purposes. We have therefore excluded this frame from our study. We have also excluded 6N15, since most of this frame is strongly foreshortened. The small portion which is not severely foreshortened reveals cratered terrain of the type covered by 6N19. Pertinent data, based on Collins (1971), for the remaining four frames are given in Table I. The pass-bands of the M6 and M7 camera filters are given by Danielson and Montgomery (1971). The M9 A-frames studied here were taken with the equivalent of an orange filter. Throughout this paper Mariner 9 pictures are identified by the orbit number on which they were taken followed by the DAS time—a unique picture identifier used during the Mariner 9 mission.

A. 6N11

This frame of the Aram/Meridiani Sinus region taken with a green filter (G) has a large amount of overlap with 6N13, taken with a red filter (R). The overlap region can be used to study the relative visibility of dark splotches on R and G frames.

As Fig. 1 shows, although the contrast of dark splotches is greater on the R-frame, they are nevertheless quite visible on the G-frame. Therefore, in the following discussion, it is fair to expect that splotches and other albedo markings should be visible on G-frames.

B. 6N13

This red filter (R) frame of the Meridiani Sinus region shows the highest contrast differences of any M6 frame. The twelve windows studied (A–L) are shown in Fig. 2. These comparisons are shown in Figs. 3–14. The Mariner 9 season covered varies from $L_s = 332°$ (Rev. 137) to $L_s = 343°$ (Rev. 180).

The major trends revealed by these comparisons can be summarized as follows:

1. Large scale changes in major albedo boundaries have occurred. (cf. C, F, K, L.)
2. In 6N13 much of the intercrater area in Meridiani Sinus was uniformly dark. In 1972 many relatively bright patches were present (C, D, E, G, H, I, J, K).
3. While in a given area some dark splotches within craters have changed, others have remained remarkably constant (D, E, K, L).
4. However, there was a trend in 1969 for the craters on the western edge of Meridiani Sinus to have uniformly dark crater floors. In 1972, many of these show splotches; that is, there is both bright and dark material on the crater floors (D, E).
5. On a small scale, some dark albedo boundaries intensified during the two-year interval, and a few new ones appeared (A, C).
6. Some bright, stubby crater streaks or tails present in 1969 remained unchanged in direction (trending south-west), and probably in appearance. Others, trending similarly, appear longer in 1972 (C, D).
7. Some new bright crater streaks, not present in 1969, appeared trending south-west (A, C, D, E).
8. A set of diffuse dark streaks, vaguely present in 1969, intensified. They show a south-westerly trend similar to that of the bright streaks mentioned above (B).
9. One dark crater splotch, visible in 1969, extended into a darkish streak (trending south-west) (A).

TABLE I

MARINER 6 A-FRAME DATA SELECTED FOR DETAILED STUDY (COLLINS, 1971)

	Filter	Range (km)	Phase angle	Lighting angle	Viewing angle	Lat/long
6N11	G	4541	51°	51°	37°	3°S, 4°W
6N13	R	4331	52°	61°	40°	4°S, 354°W
6N19	G	3617	80°	59°	25°	17°S, 357°W
6N11	R	3501	80°	70°	17°	16°S, 345°W

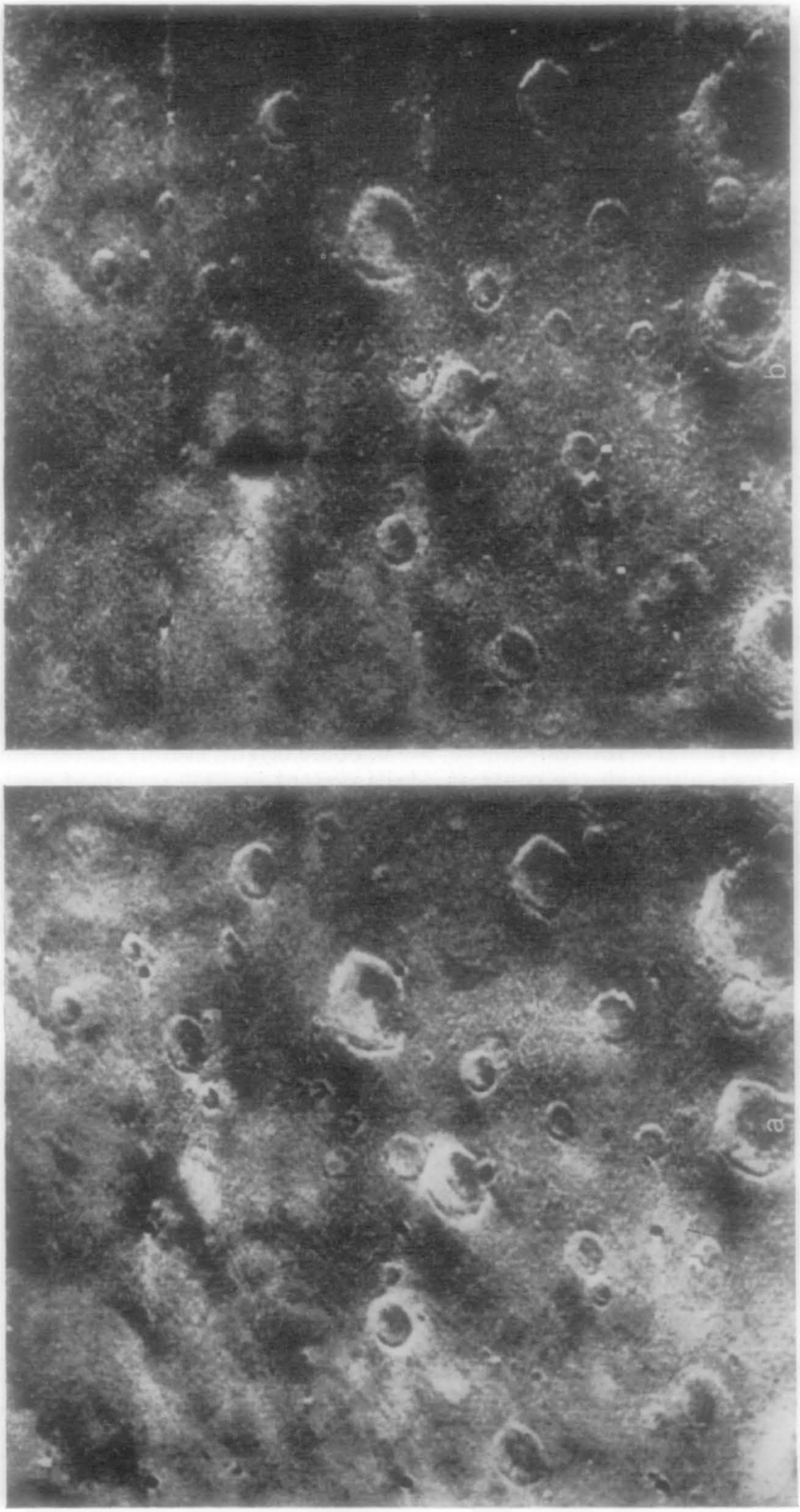

FIG. 1. A comparison of parts of: (a) 6N13, taken with a red filter; and (b) 6N11, taken with a green filter—showing the relative contrast of dark crater splotches in the two colors. The dark spot in the upper left quadrant of 6N11 is a camera blemish.

FIG. 2. Frame 6N13, showing the various windows studied.

10. A new set of small crater-associated bright streaks appeared, trending south-east. These were definitely not present in 1969 (H, I, J, K).

C. 6N19

This G frame covers the bright region Deucalionis Regio and its boundary with Sinus Meridiani. A few darkish splotches are visible in the original frame. Five windows contained in this frame were compared with Mariner 9 data (Fig. 15). Three of these comparisons are shown in Figs. 16–18. The seasonal range covered by the M9 pictures correspond to $L_s \simeq 332°$ to $343°$.

The principal findings based on 6N19 can be summarized as follows:

1. Many dark crater splotches, not present in 1969, are seen in the M9 pictures (A, B, D).
2. Several dark streaky splotches outside of craters have appeared (B).
3. At least one small bright crater-associated streak (trending north-east) has appeared (cf. arrow in Fig. 17).

D. 6N21

This R-frame covers Sabeus Sinus and

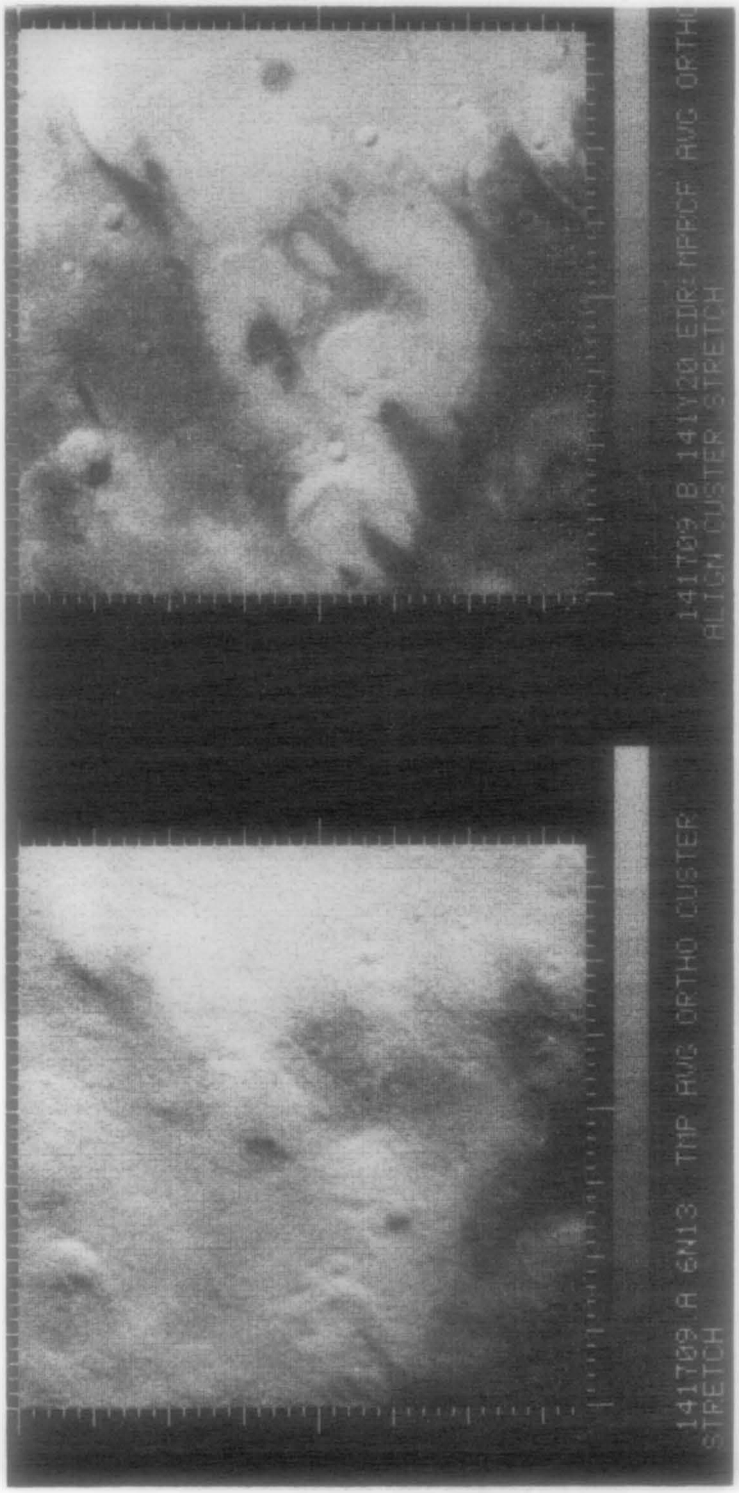

FIG. 3(a). Window A with R 141/663313. Contrast stretched.

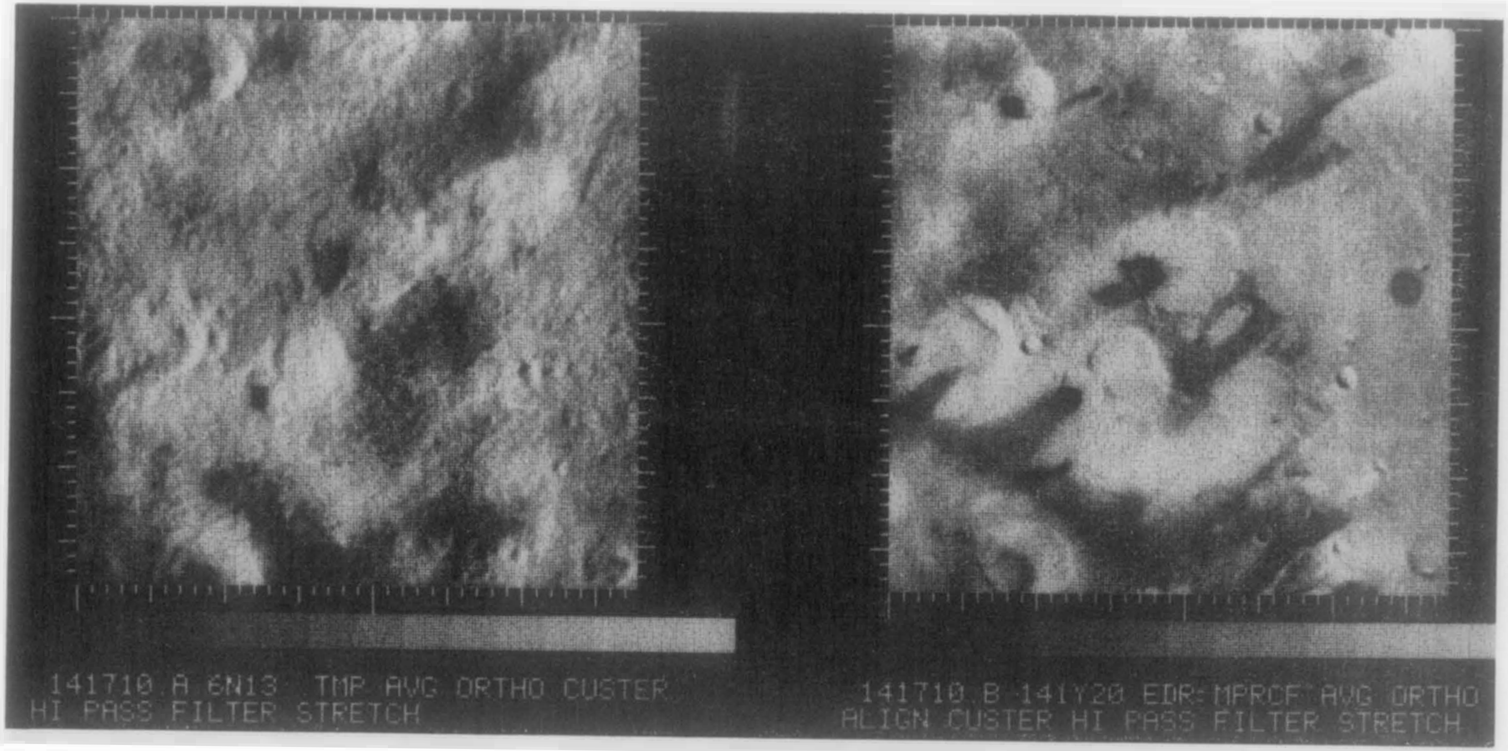

FIG. 3(b). Window A with R 141/663313. High pass filtered and contrast stretched. Numerous changes are visible. Note the development of a dark albedo boundary; the growth of a dark streak out of a dark crater splotch; and the appearance of at least one crater-associated white tail. (K = 1.65.)

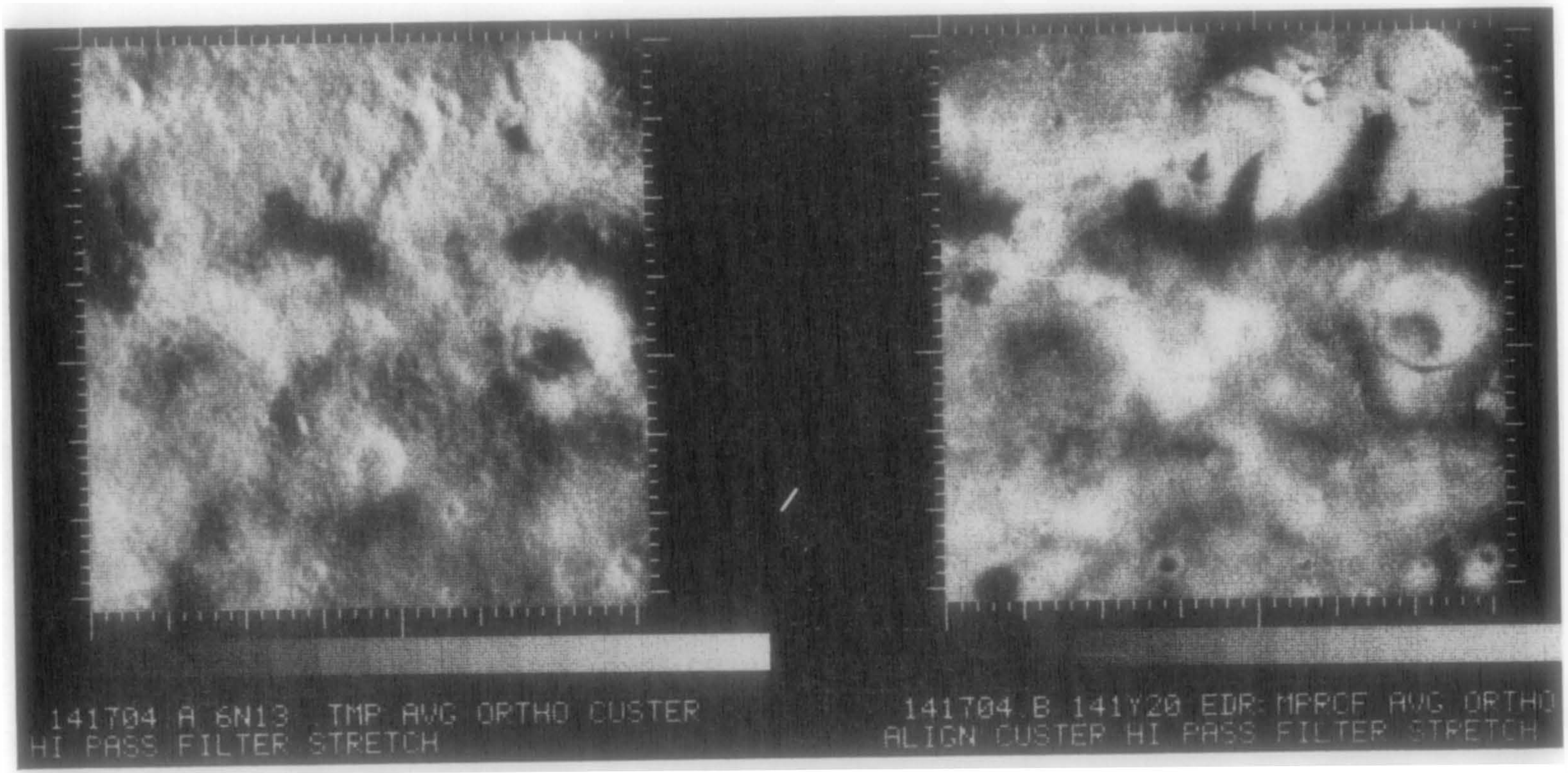

FIG. 4. Window B with R 141/6643313. High pass filtered and contrast stretched. This comparison shows the development of several dark streaks, which blend into an albedo boundary. One of these streaks is obviously related to a crater splotch (cf. Fig. 3). ($K = 1.60$.)

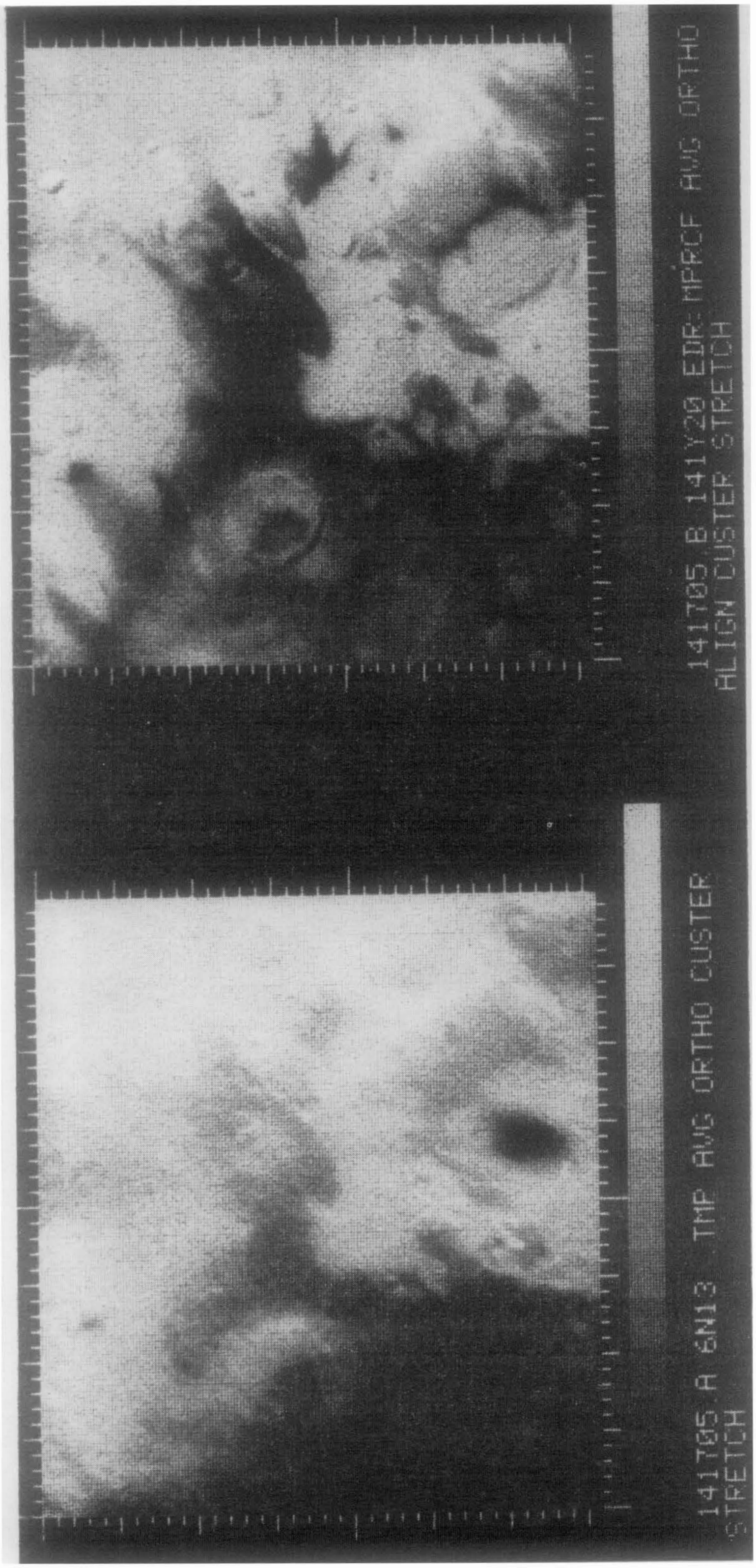

FIG. 5(a). Window C with R141/6643313. Contrast stretched.

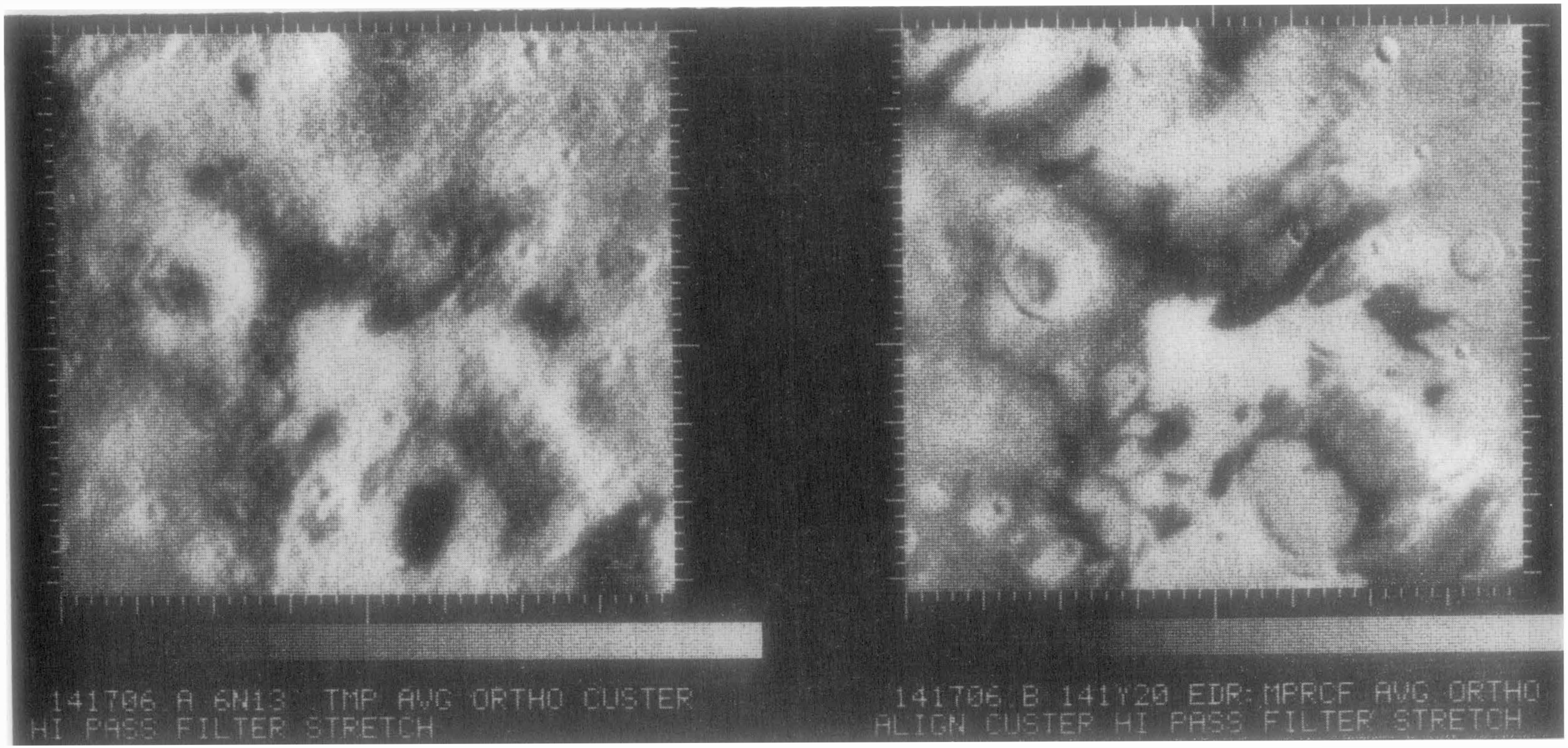

FIG. 5(b). Window C with R141/6643313. High pass filtered and contrast stretched. The M6 window contains a large, dark, camera blemish (lower right). The outline of at least one dark splotch has changed. The albedo boundary running diagonally to the upper left is reinforced in the M9 view. White crater-associated tails are present in both. ($K = 1.60$.)

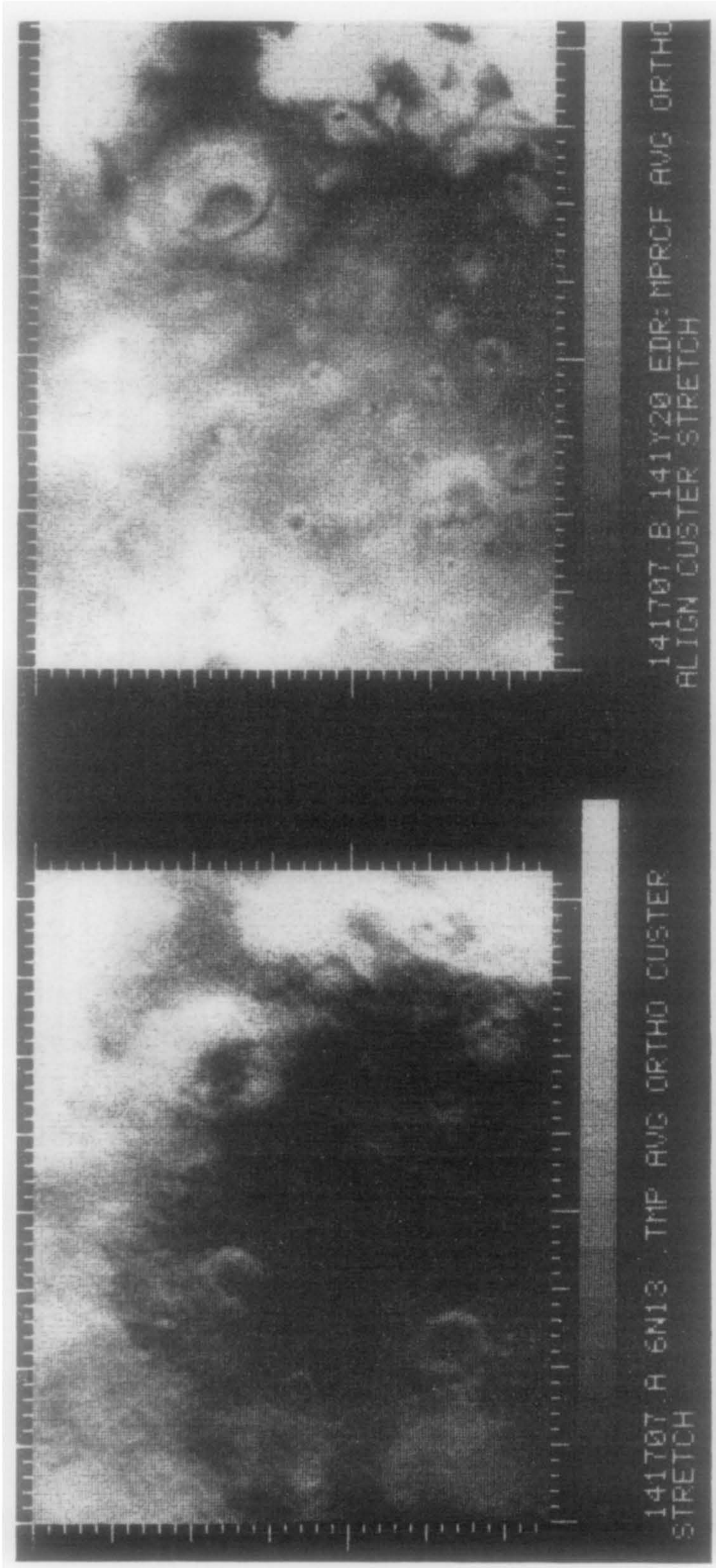

FIG. 6(a). Window D with R141/6643313. Contrast stretched.

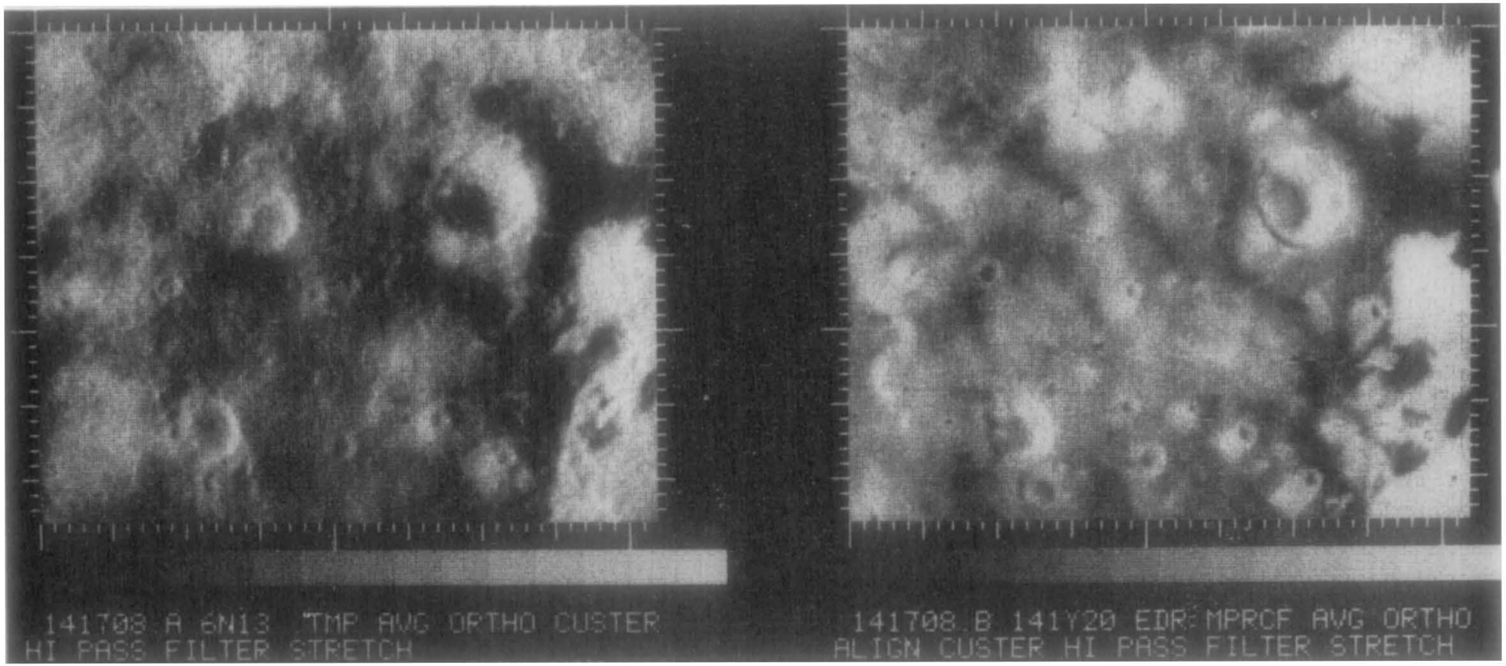

FIG. 6(b). Window D with R141/6643313. High pass filtered and contrast stretched. Some craters which were uniformly dark in 1969, have floor splotches in 1971. In addition, much intercrater brightening has occurred since 1969. Note the prominent change in the albedo boundary and the enhancement of the bright crater tails at lower right. ($K = 1.60$.)

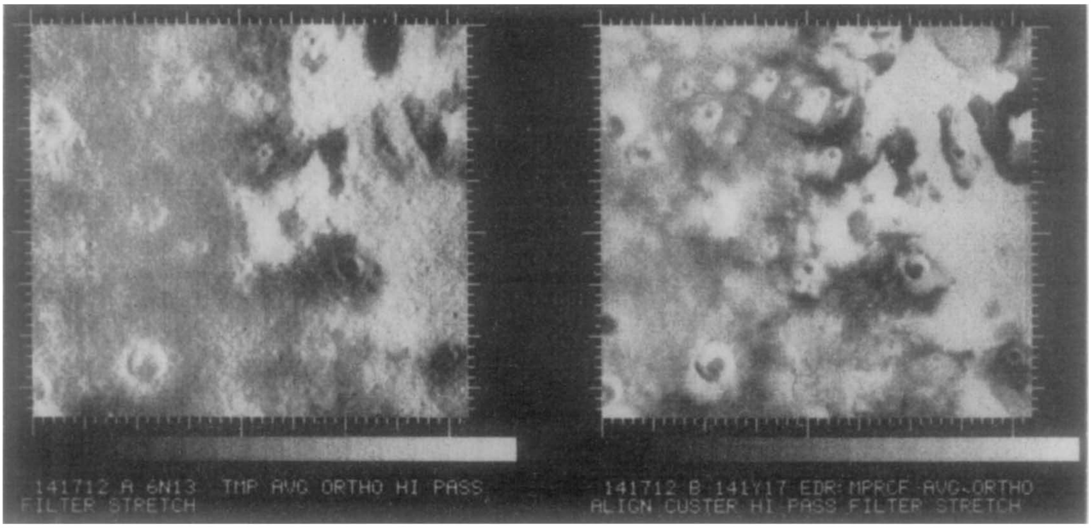

FIG. 7(a). Window E with R141/6642968. Contrast stretched.

Deucalionis Regio. The locations of the various comparison windows are shown in Fig. 19. Unlike 6N13 this Mariner 6 frame shows little albedo detail. The eight comparisons are shown in Figs. 20–27, and the principal conclusions can be summarized as follows:

1. Prominent and extensive albedo boundaries have appeared in this area (A, B, C).
2. No contrast changes have occurred in some nearby areas (E).
3. Many dark crater splotches have appeared (A, B, C).

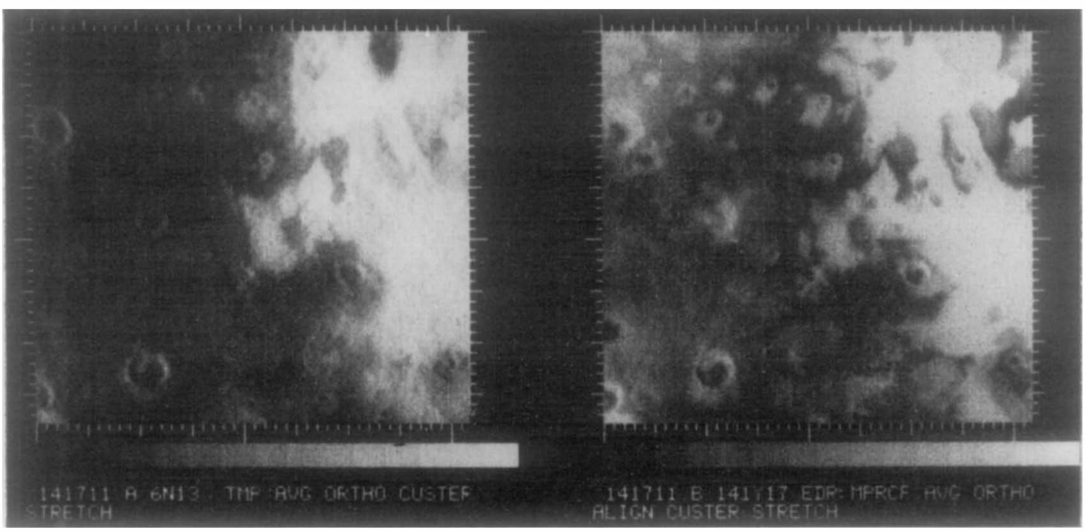

FIG. 7(b). Window E with R141/6642968. High pass filtered and contrast stretched. This comparison confirms that there were many more relatively bright patches both in and out of craters in 1971 than in 1969. A number of craters which had unformly dark crater floors in 1969 now have splotches. A set of stubby bright crater tails are present in both views (although perhaps more developed in 1971) indicating the constancy of prevailing winds. ($K = 1.62$.)

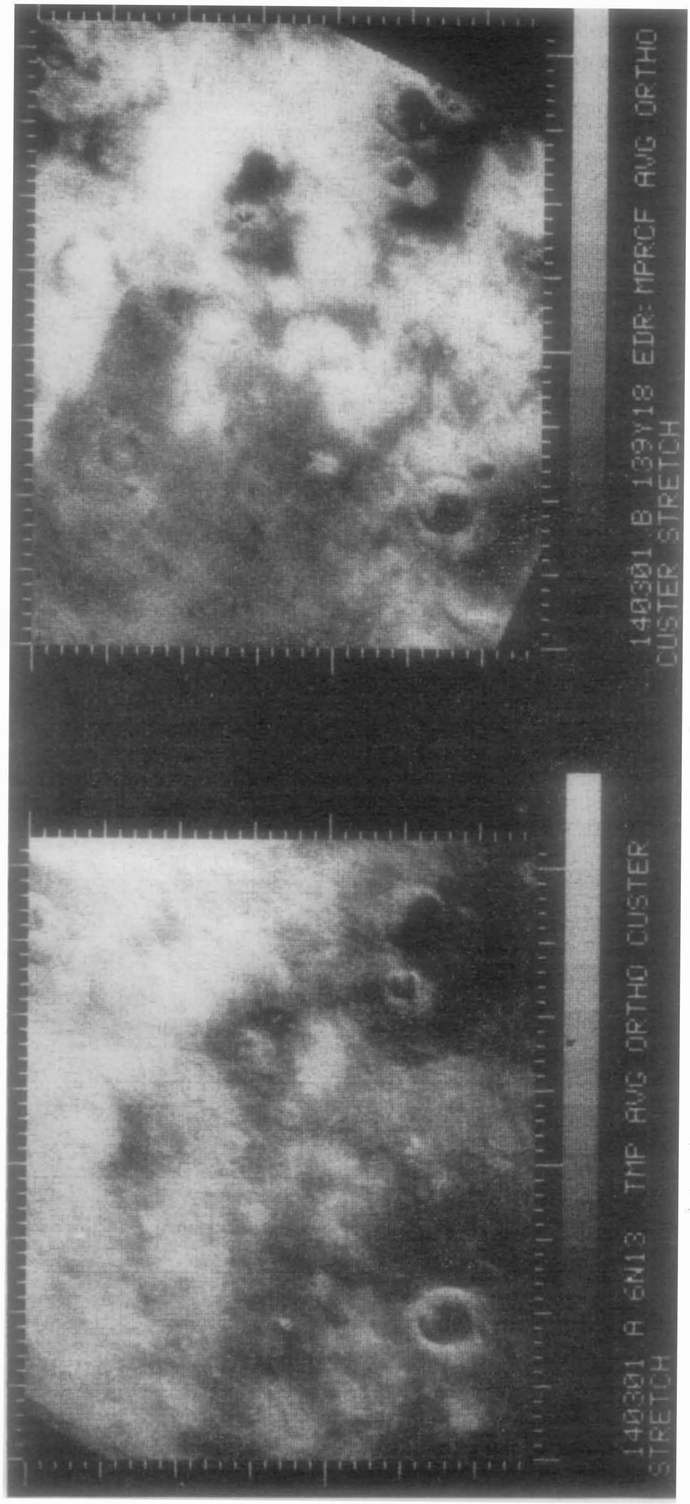

FIG. 8. Window F with R139/6571353. Contrast stretched. A good example of large scale changes in albedo boundaries. There may be an indication of a change in direction of a white tail (left of center). ($K = 1.80$.)

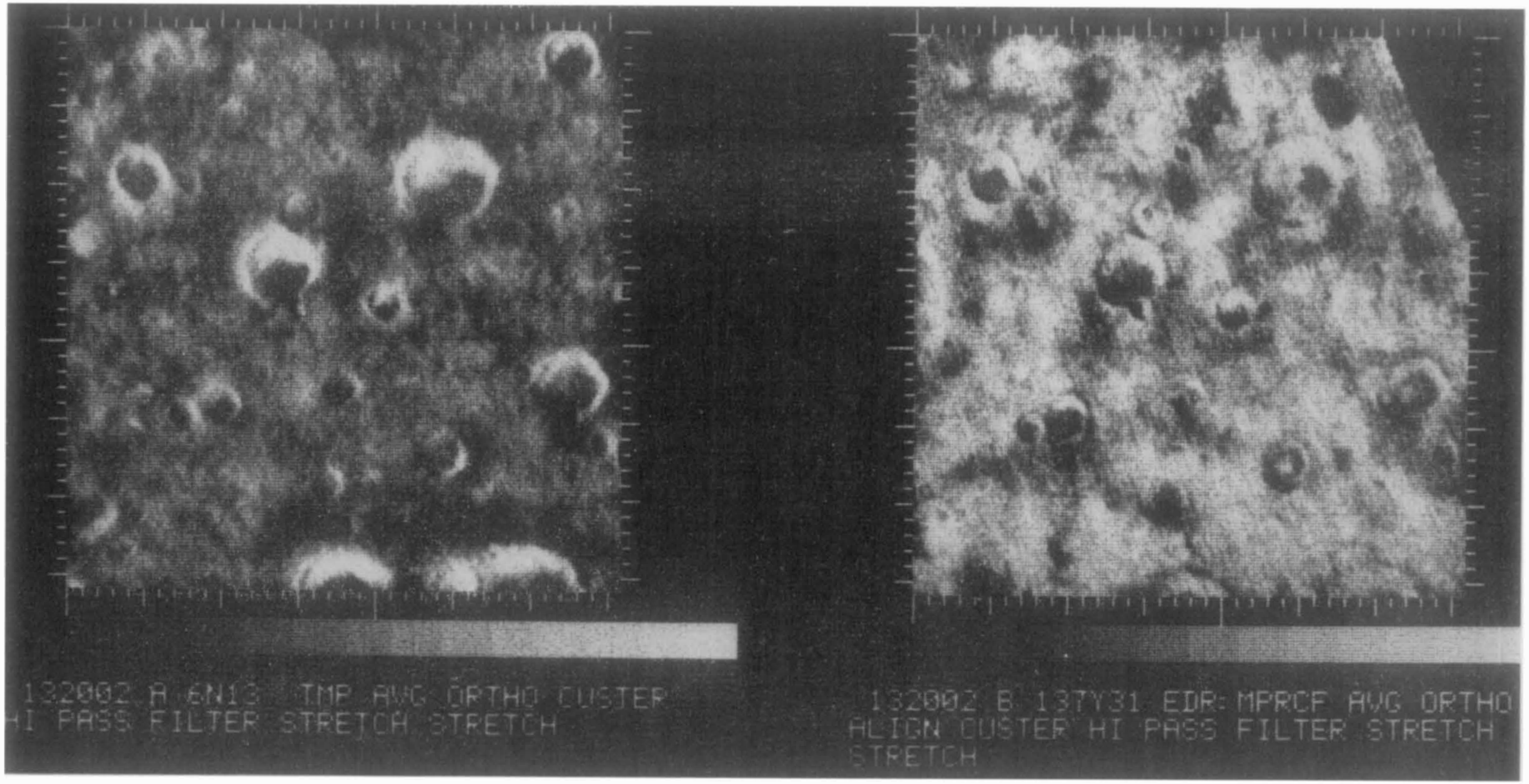

Fig. 9. Window G with R137/6499673. High pass filtered and contrast stretched. Large changes in albedo boundaries are visible. In 1969 the intercrater area was more uniformly dark than in 1971. In some of the craters changes in splotch outlines have occurred. The dark spot in the upper right corner of the M9 window is a camera blemish. ($K = 2.20$.)

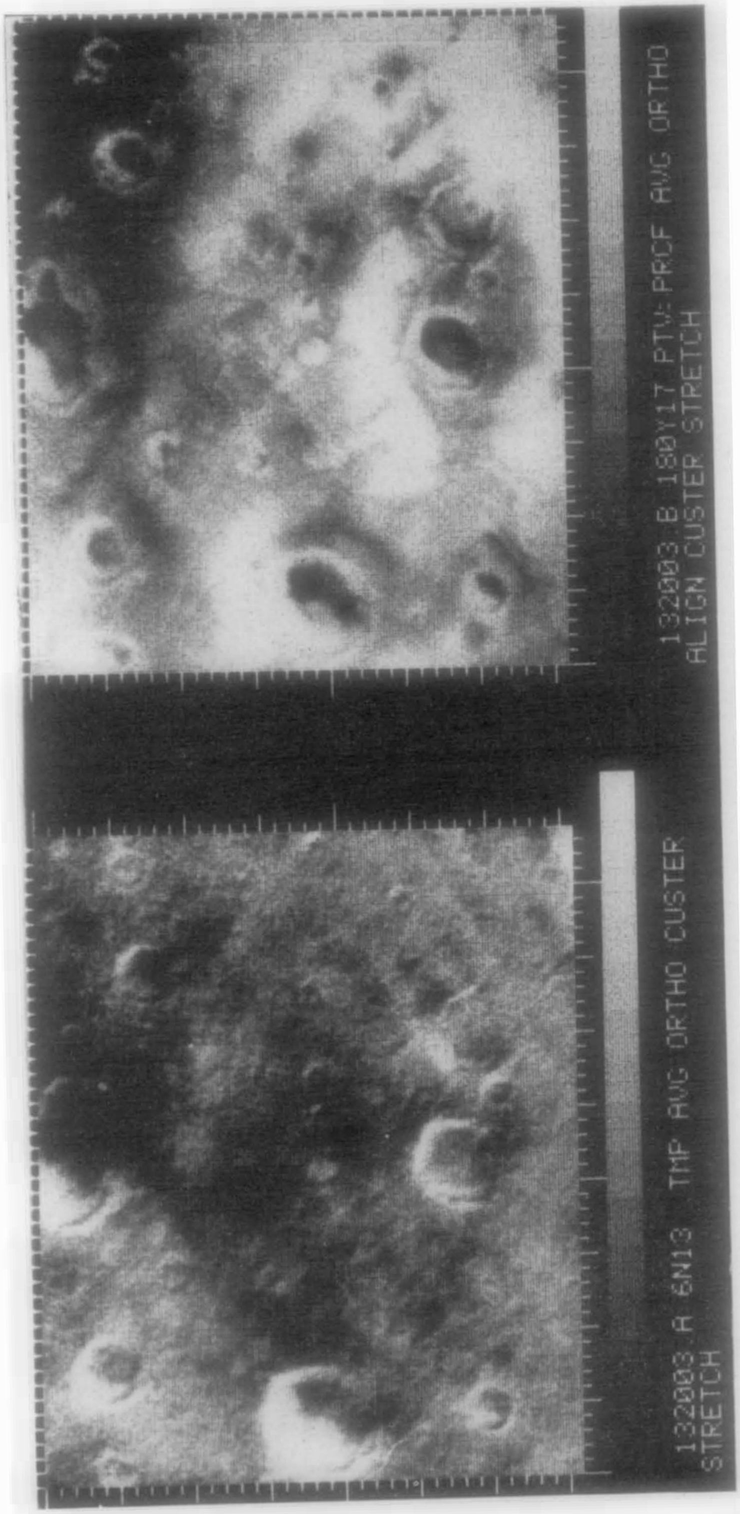

FIG. 10(a). Window H with R180/8045763. Contrast stretched.

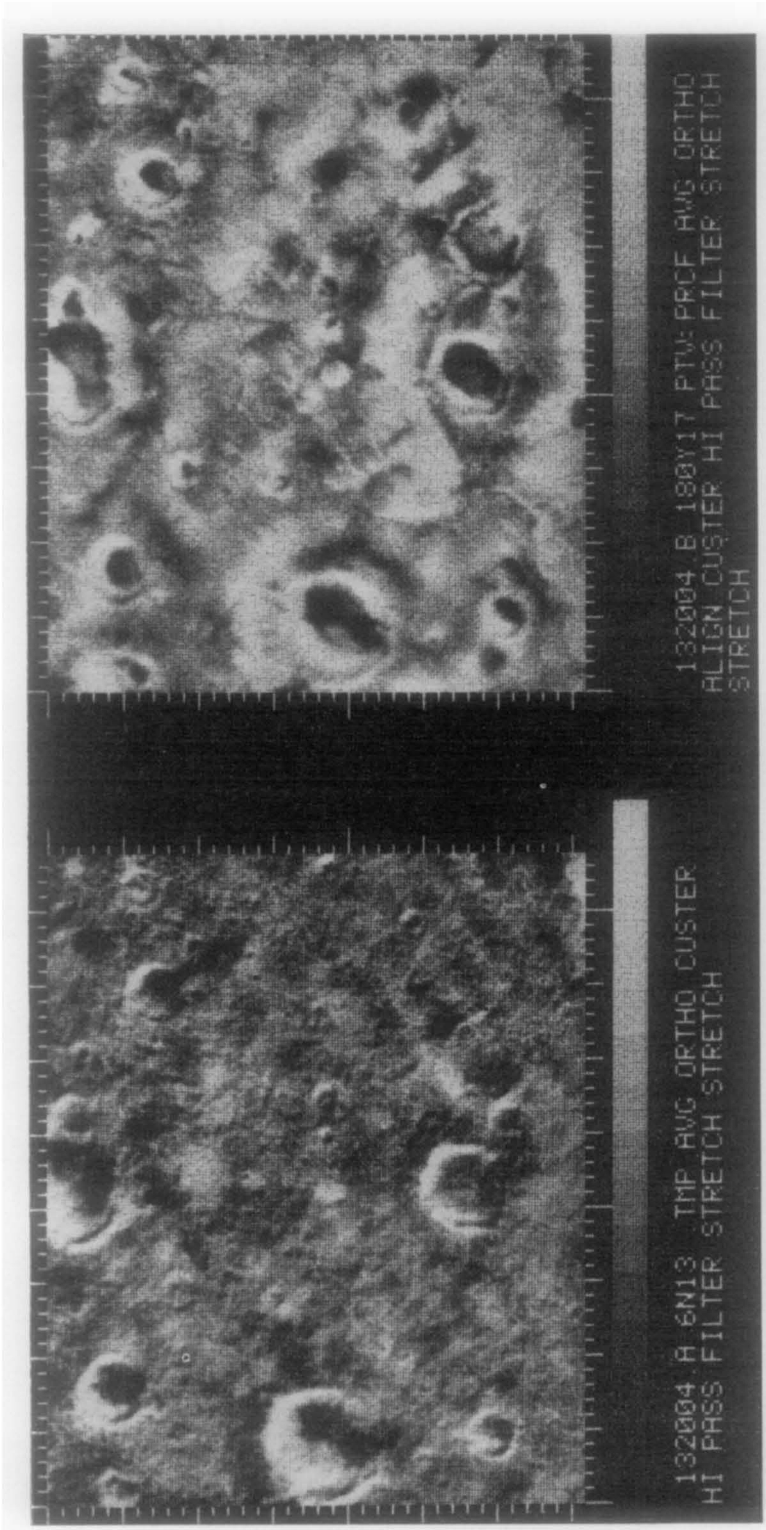

FIG. 10(b). Window H with R180/8045763. High pass filtered and contrast stretched. One of the best examples of the appearance of a large bright area in inter-crater region in 1971. Note the development of a bright stubby crater tail trending to the right (center). ($K = 1.70$.)

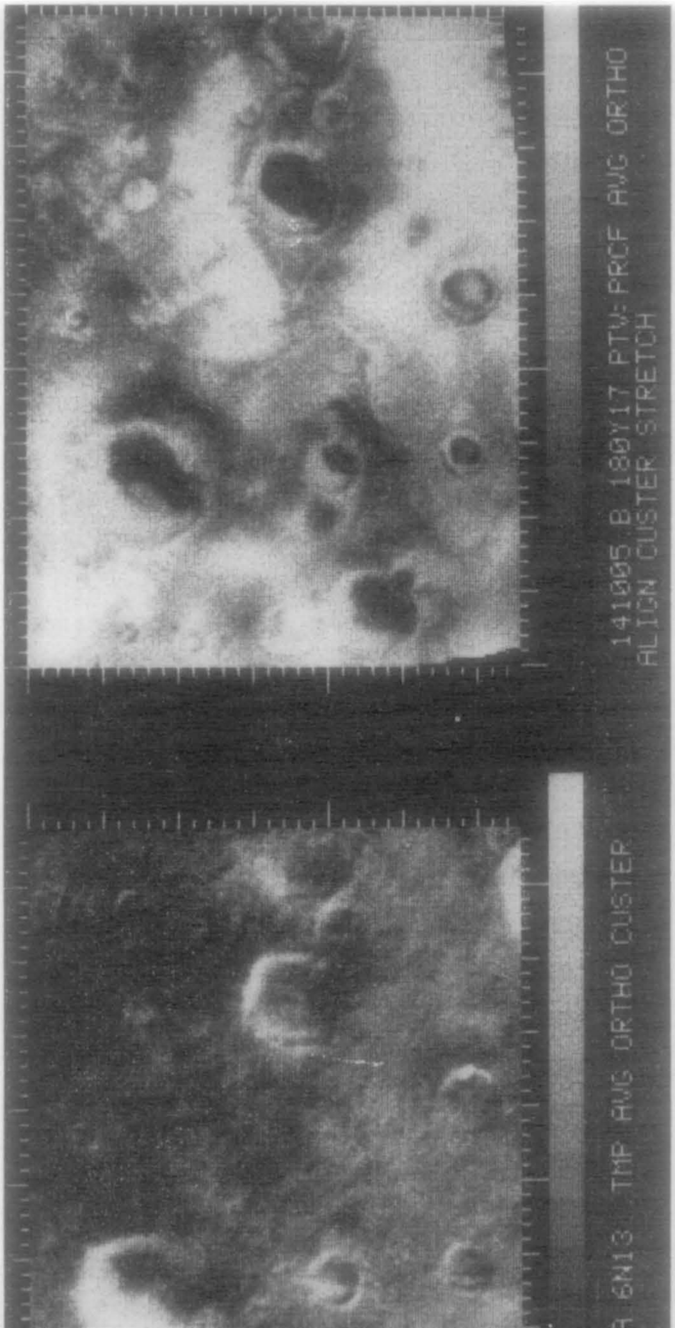

FIG. 11(a). Window I with R180/8045763. Contrast stretched.

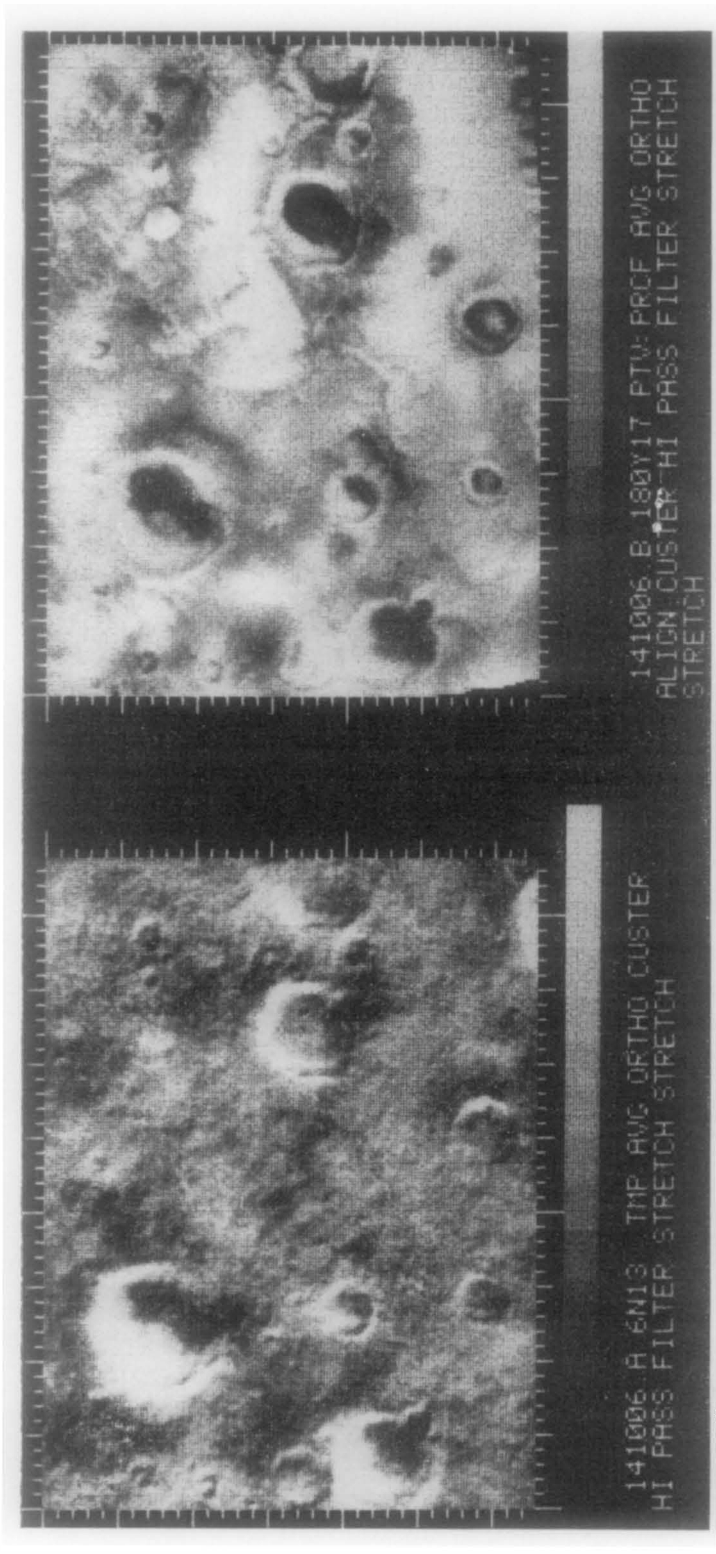

FIG. 11(b). Window I with R180/8045763. High pass filtered and contrast stretched. A window similar to H, but at somewhat higher resolution. ($K = 1.50$.)

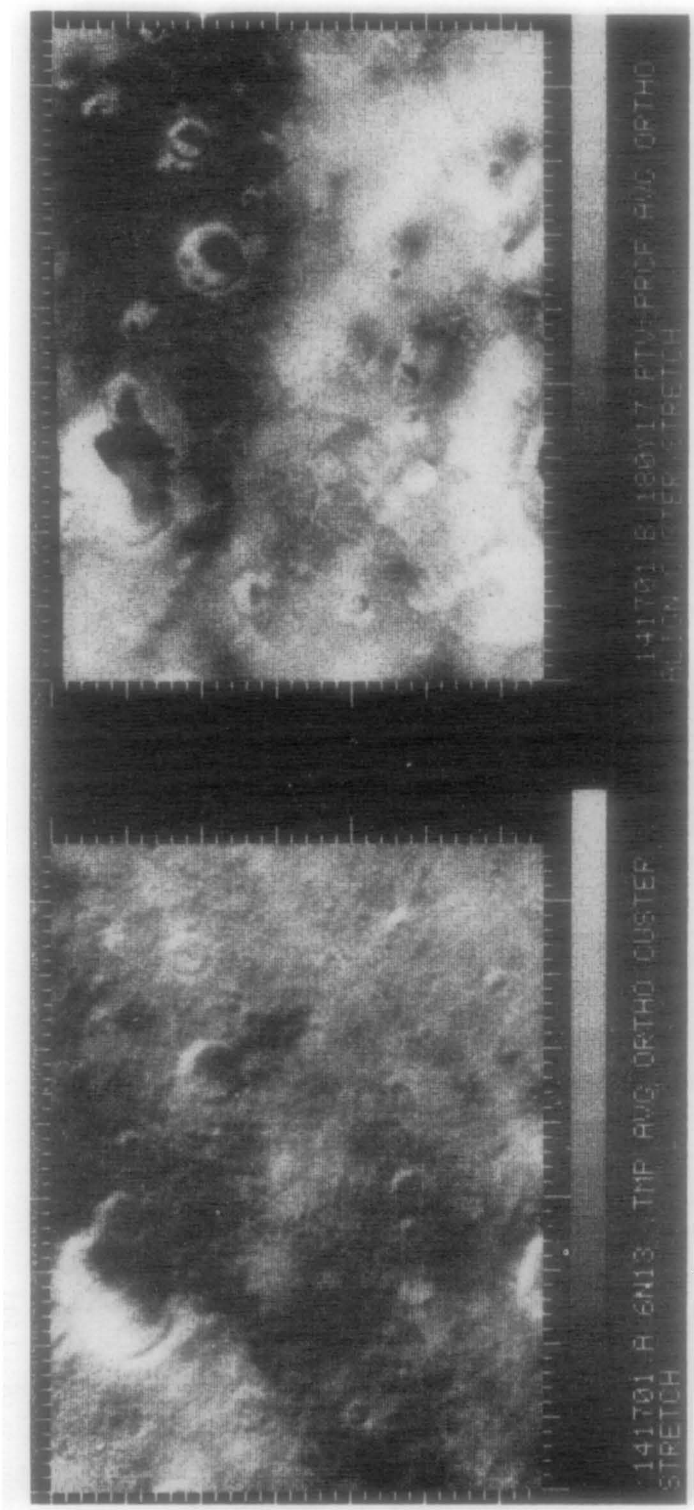

FIG. 12(a). Window J with R180/8045763. Contrast stretched.

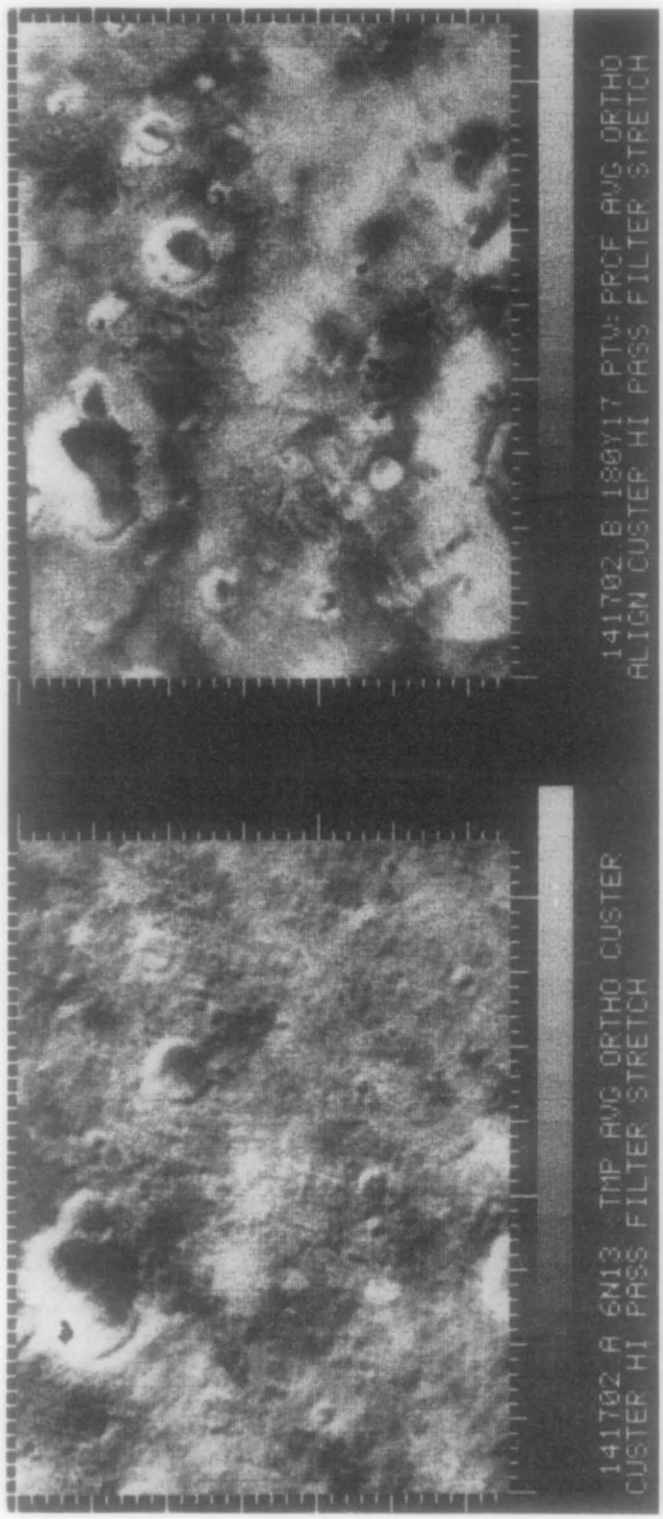

FIG. 12(b). Window J with R180/8045763. High pass filtered and contrast stretched. The general inter-crater brightening is again evident. The M9 picture shows the development of two systems of white crater tails not present in 1969. ($K = 1.50$.) The dark spot in the multiple crater near the top of the M6 window is a processing blemish.

12

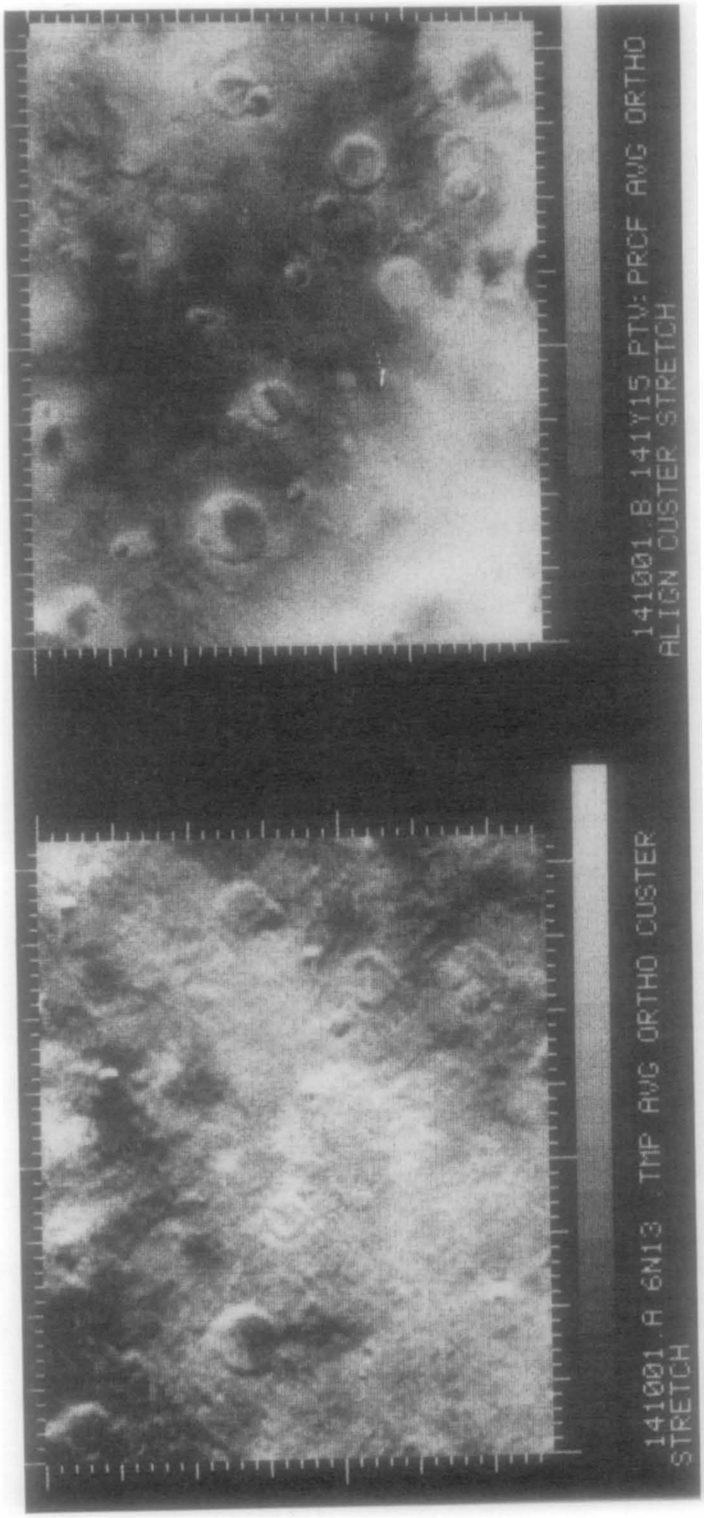

Fig. 13. Window K with R141/664893. Contrast stretched. Changes in crater splotches and the growth of a white crater tail at upper left are evident. An albedo boundary has developed at lower left. ($K = 1.40$.)

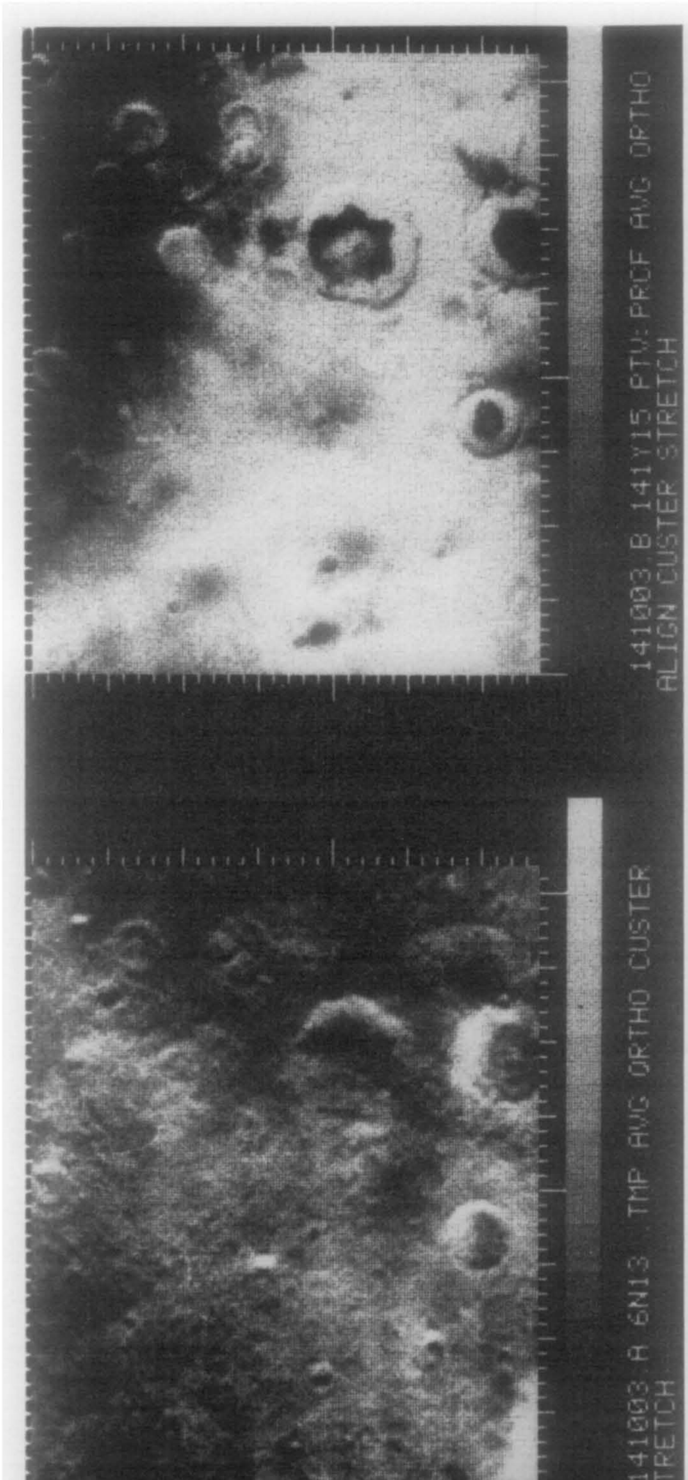

FIG. 14(a). Window L with R 141/6642893. Contrast stretched.

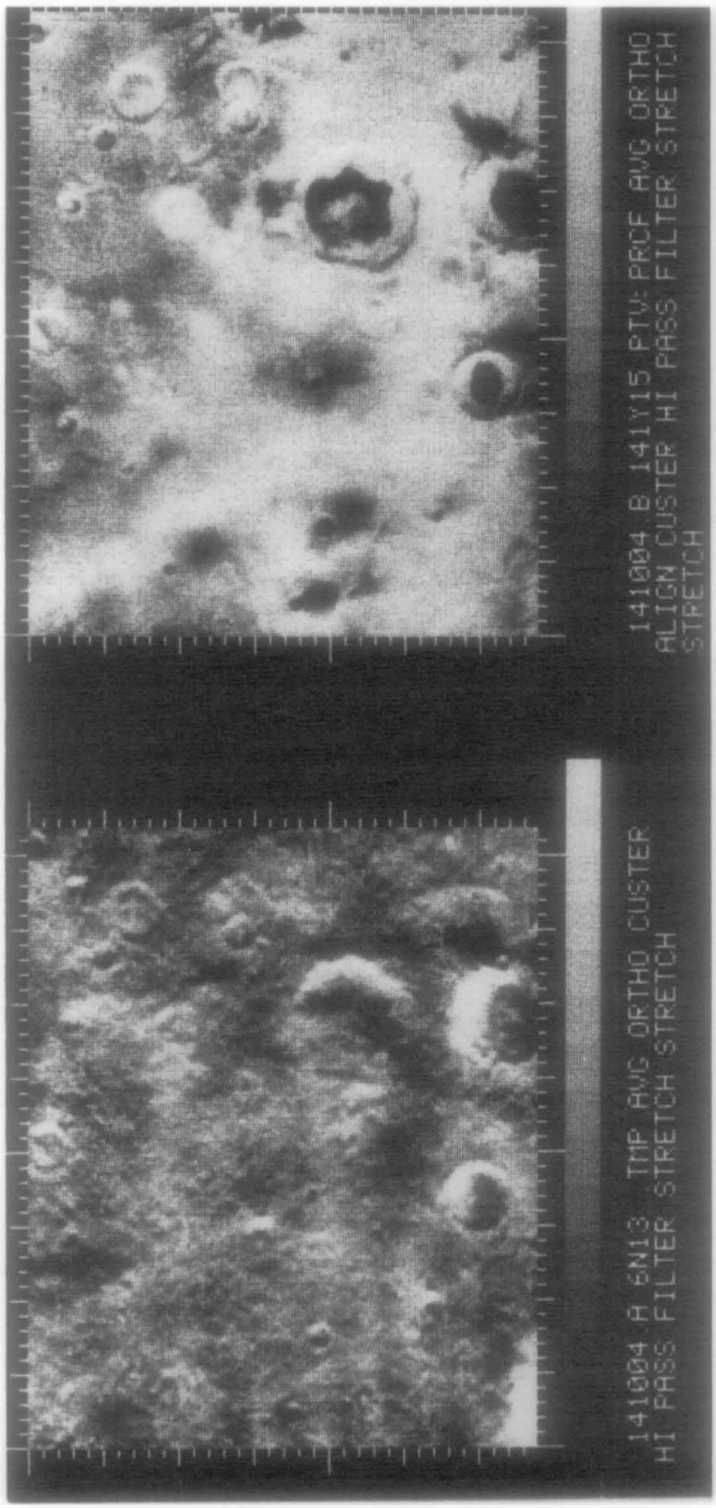

FIG. 14(b). Window L with R141/6642893. High pass filtered and contrast stretched. This comparison reveals a spectacular albedo boundary change, as well as splotch changes within craters. Especially interesting is the change in the splotches in the crater at lower right. ($K = 1.40$.)

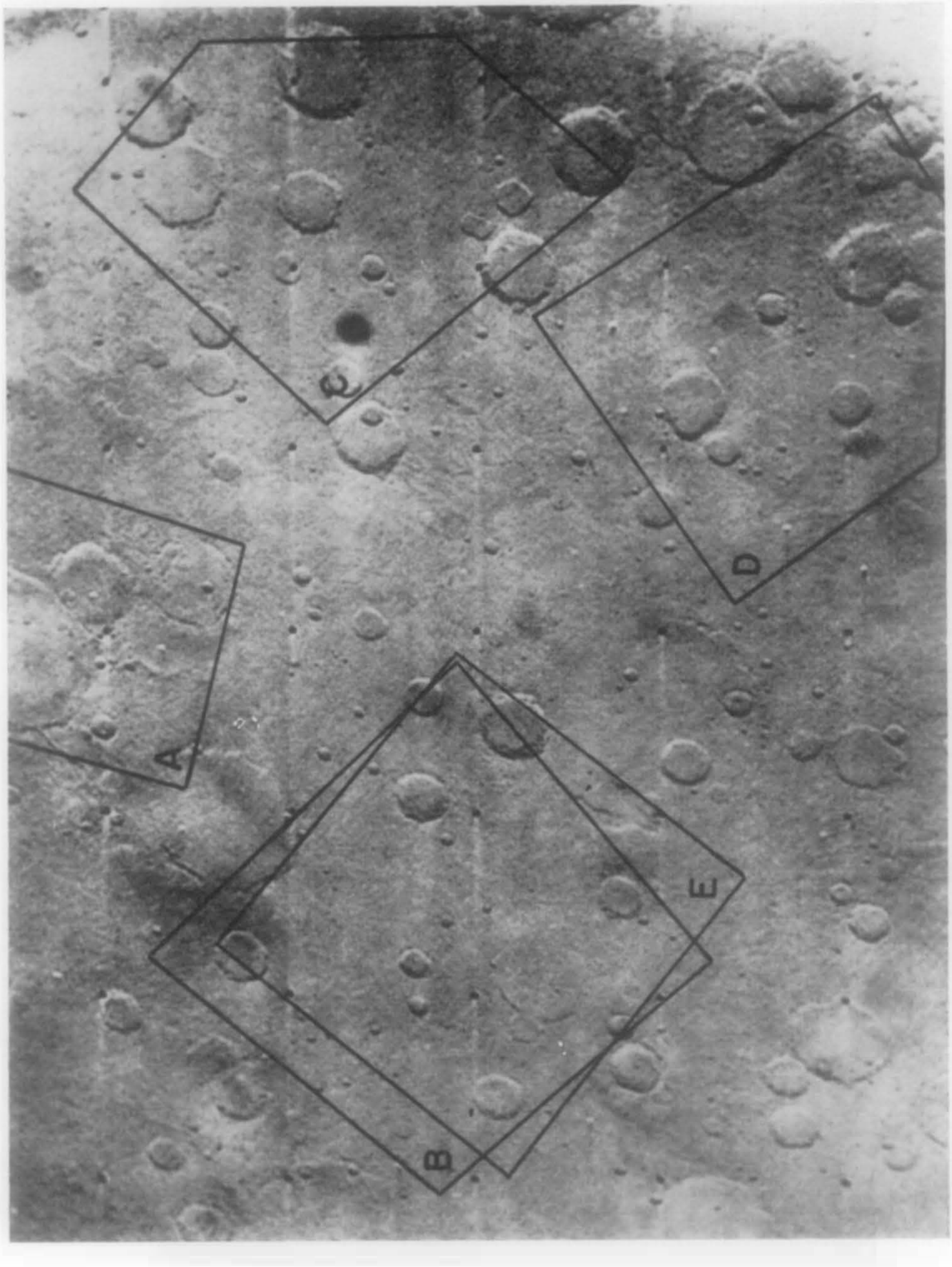

FIG. 15. Frame 6N19, showing the various windows studied.

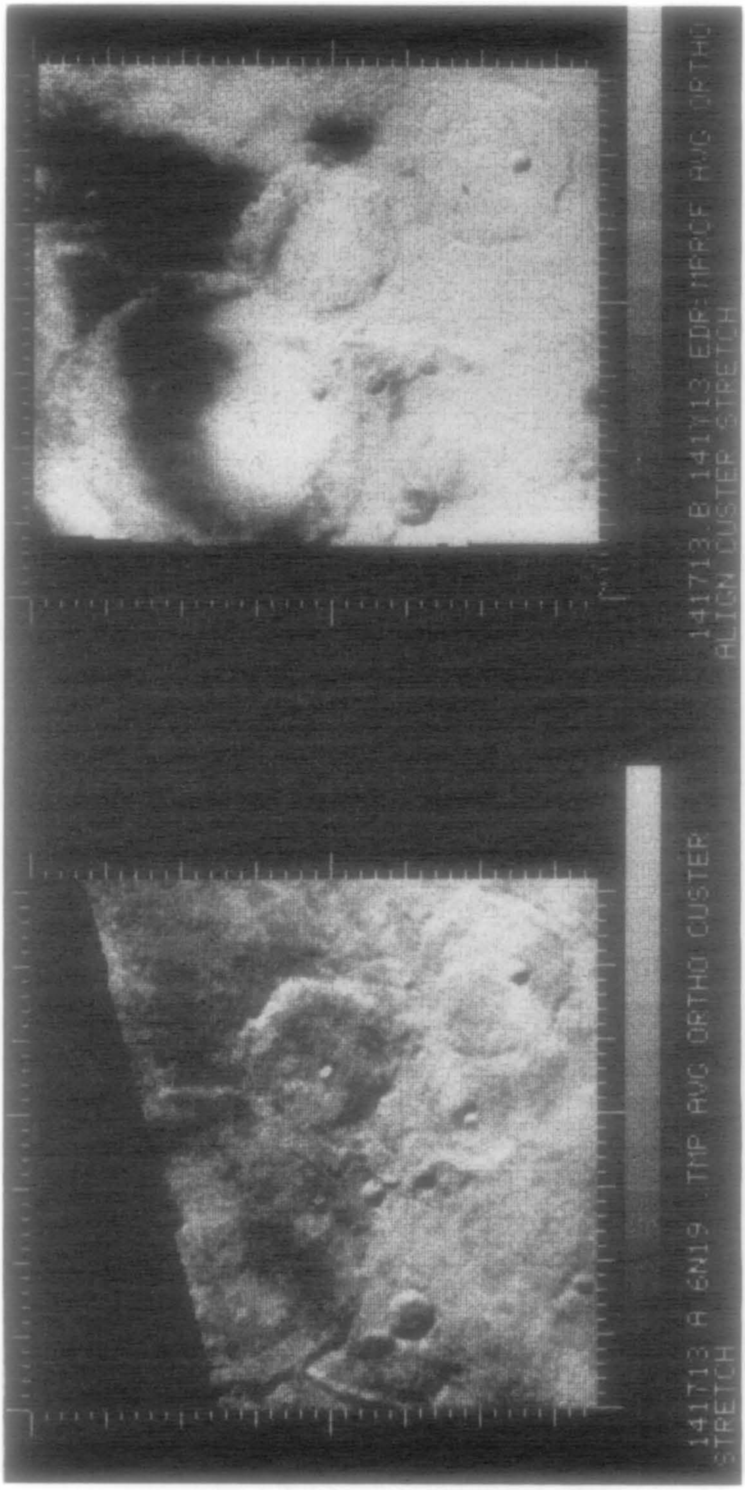

FIG. 16. Window A with R141/6642823. Contrast stretched. Whereas the M6 window is bland, considerable contrast exists in the M9 view. Extensive albedo differences have appeared both on the floor of the large crater, and on the surrounding terrain. ($K = 1.40$.)

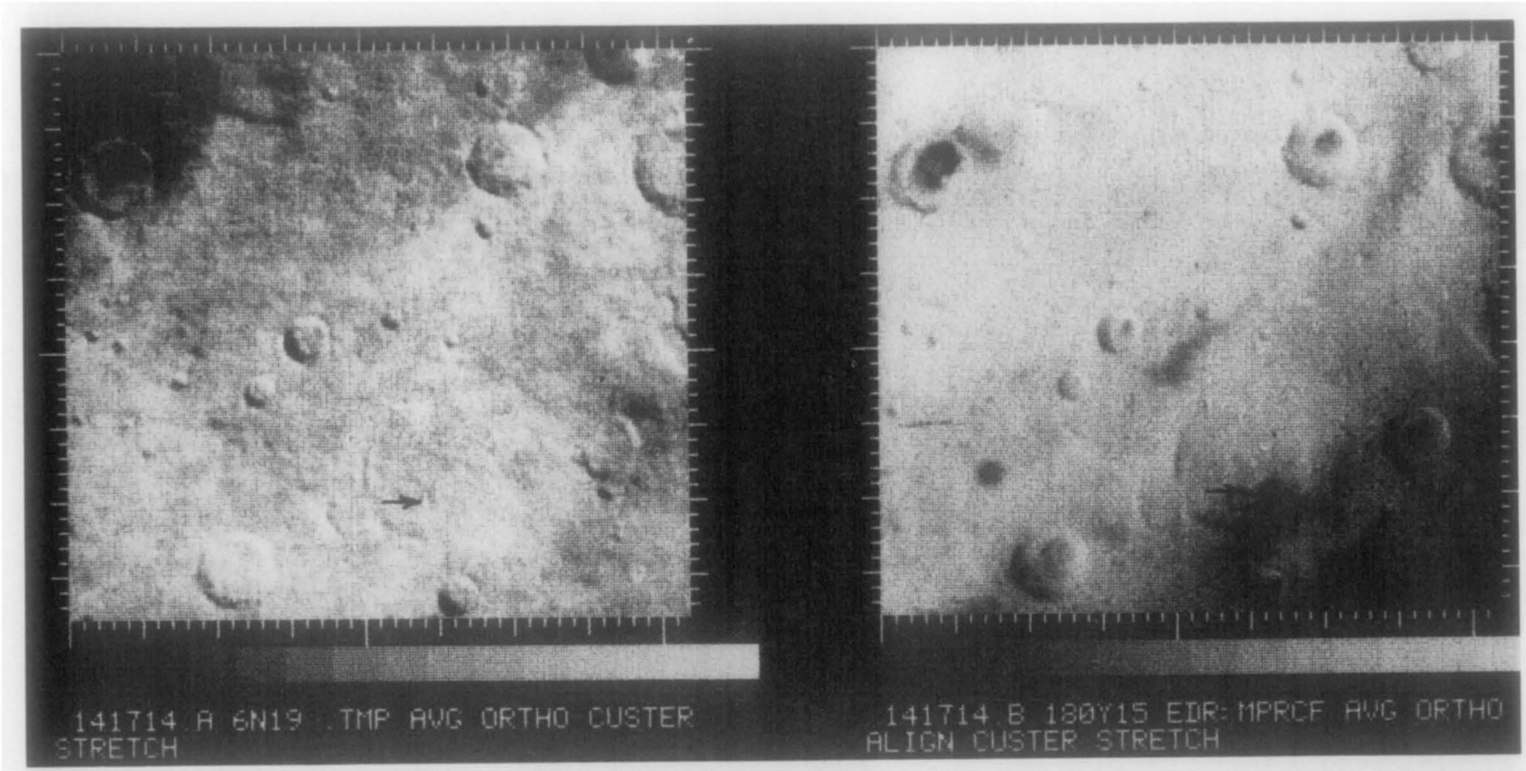

FIG. 17. Window B with R180/8045623. Contrast stretched. This comparison reveals the appearance of dark crater splotches in many of the craters, as well as several dark streaky splotches in lower right of the Mariner 9 window. The dark splotch within the crater at upper left has remained remarkably stable. There was an extensive dark area in the region above this crater in 1969, which was not there in 1971. The arrow points to a small crater from which, in the M9 view, a faintly visible bright streak emanates, trending in the direction of the upper right corner (northeast). The dark spot in the lower left corner of the M9 window is a camera blemish. ($K = 1.80$.)

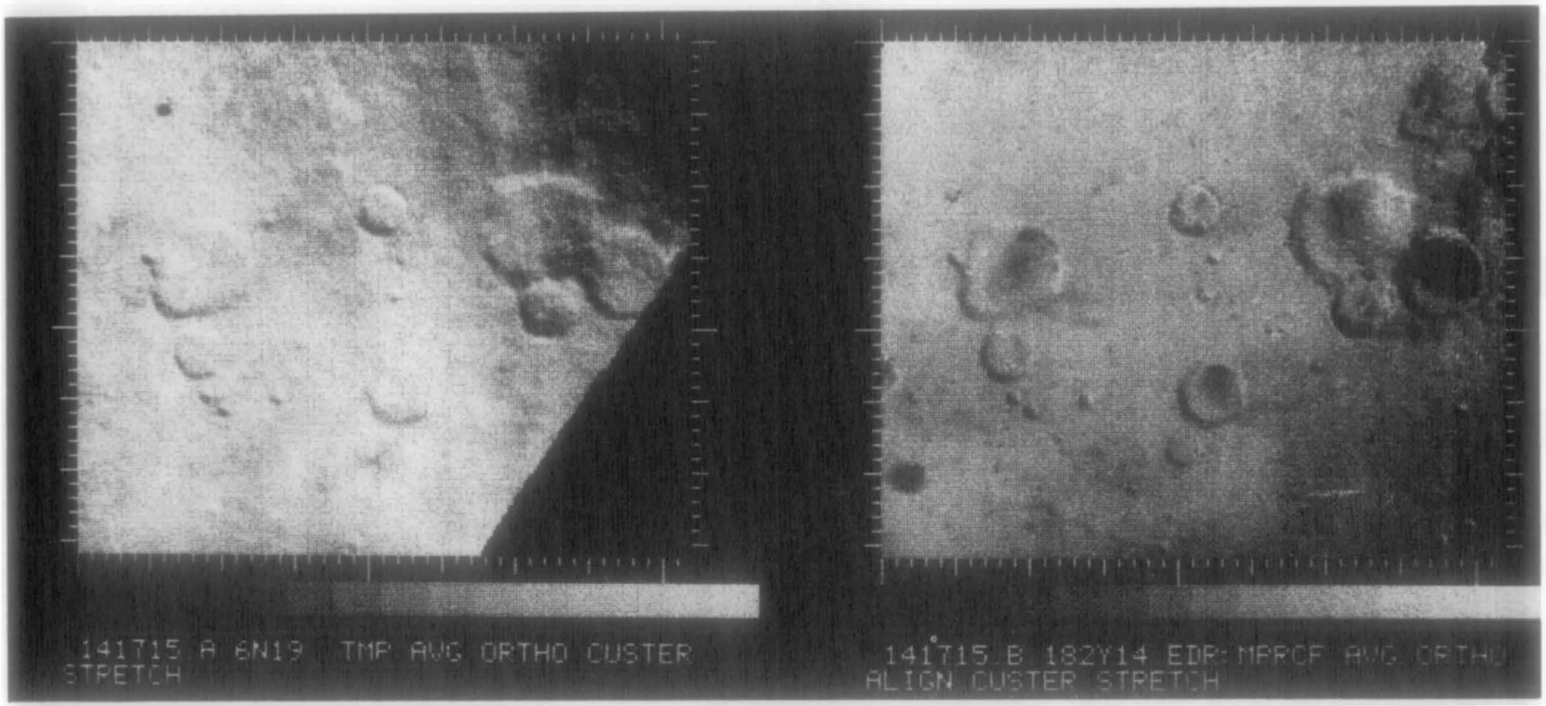

FIG. 18. Window D with R182/8117443. Contrast stretched. The M9 frame shows many dark crater splotches, not evident in 1969. The dark round spot in the lower left corner of the M9 frame is a camera blemish. ($K = 1.50$.)

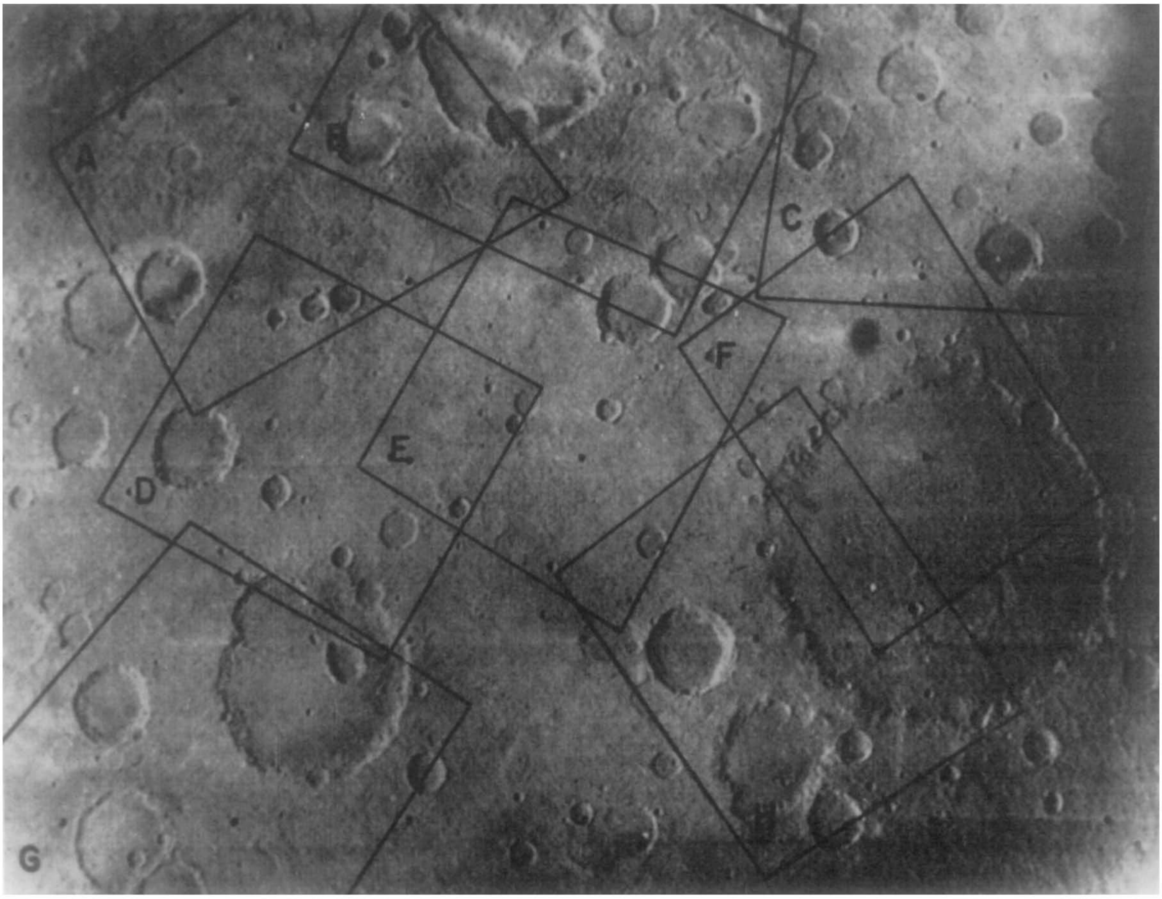

FIG. 19. Frame 6N21, showing the various windows studied.

4. In a few cases dark splotches against crater walls, not present in 1969, have appeared (H).

5. Two sets of small, bright crater tails, not present in 1969, are seen in the M9 pictures (C). One group trends south-east, the other east. Additional members of the latter group are seen in F.

6. In the same region dark streaky splotches trending south-east are present in the M9 frames, but not in 6N21 (C).

II: MARINER 7 A-FRAMES

Of the nonpolar M7 close-encounter A-frames, those up to and including 7N9 are strongly foreshortened, making them difficult to compare with Mariner 9 data.

Frames 7N11 (G) and 7N13 (R) cover the polar cap edge and provide the only means of studying the high southern latitudes not covered by frost. Unfortunately, both frames have strong residual images and are therefore not suitable for detailed analysis. Of the remaining nonpolar A frames, 7N23(G) and 7N27(G) are discussed below; 7N25 is a blue frame, and as such is excluded; 7N29 (R) shows an essentially featureless region within Hellas; 7N31 is too close to the terminator to be useful. Information about some of these frames is gathered in Table II (cf. Collins, 1971).

A. 7N11

This frame has severe residual image problems, and is therefore not worth

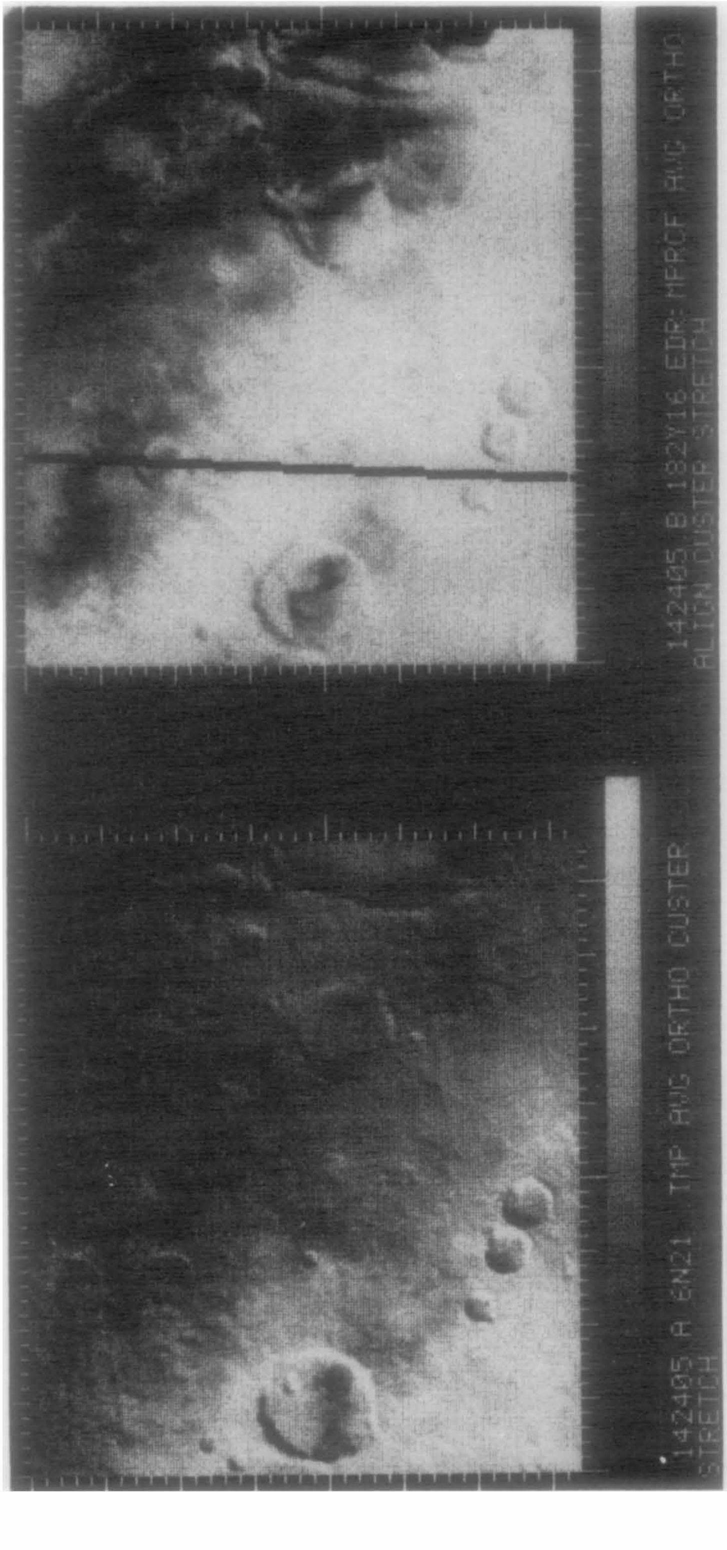

FIG. 20. Window A with R182/8117583. Contrast stretched. Note the formation of an albedo boundary running diagonally across the picture, and the associated appearance of many dark crater splotches in the **M9** picture. The position of the dark splotch in the large crater on the left differs in the two views. ($K = 1.65$.)

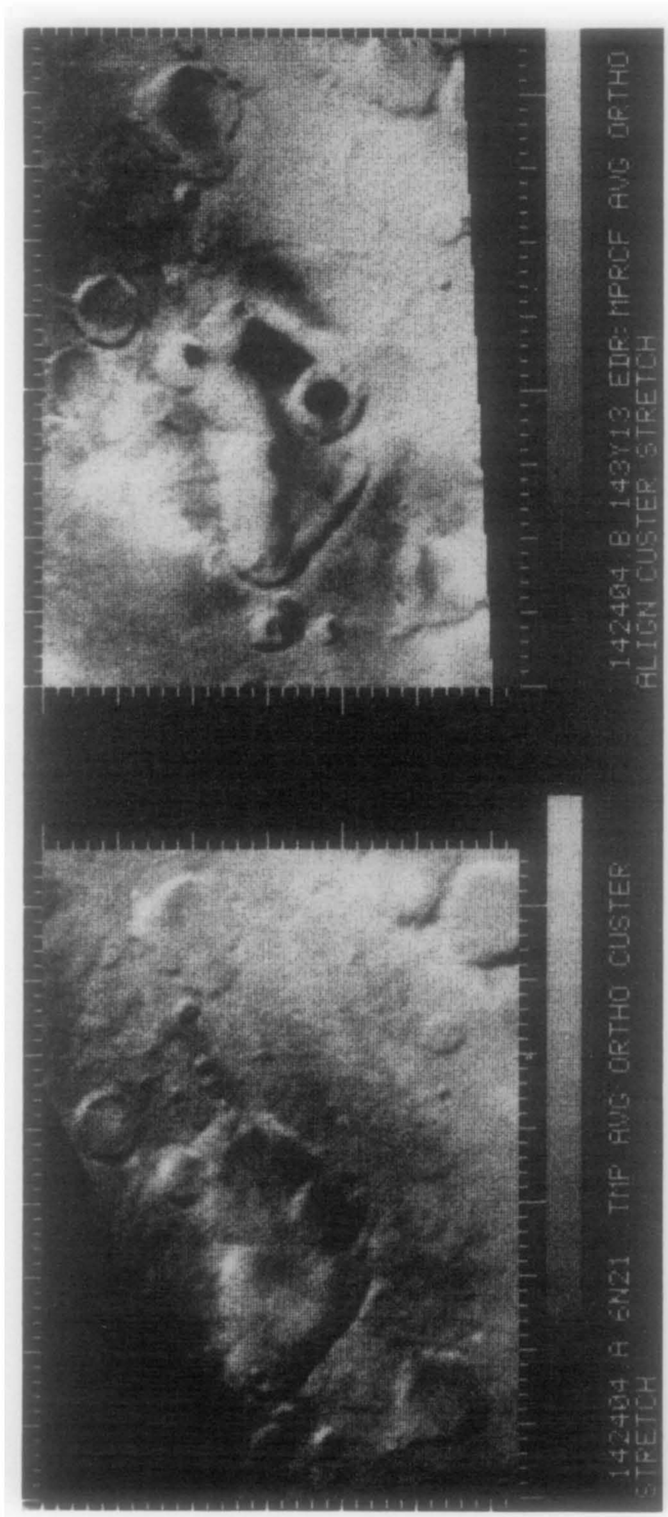

FIG. 21. Window B with R143/6714783. Contrast stretched. An example of the great increase in contrast differences in the M9 picture. Note especially the appearance of the prominent albedo boundary within the heart-shaped crater. ($K = 1.75$.)

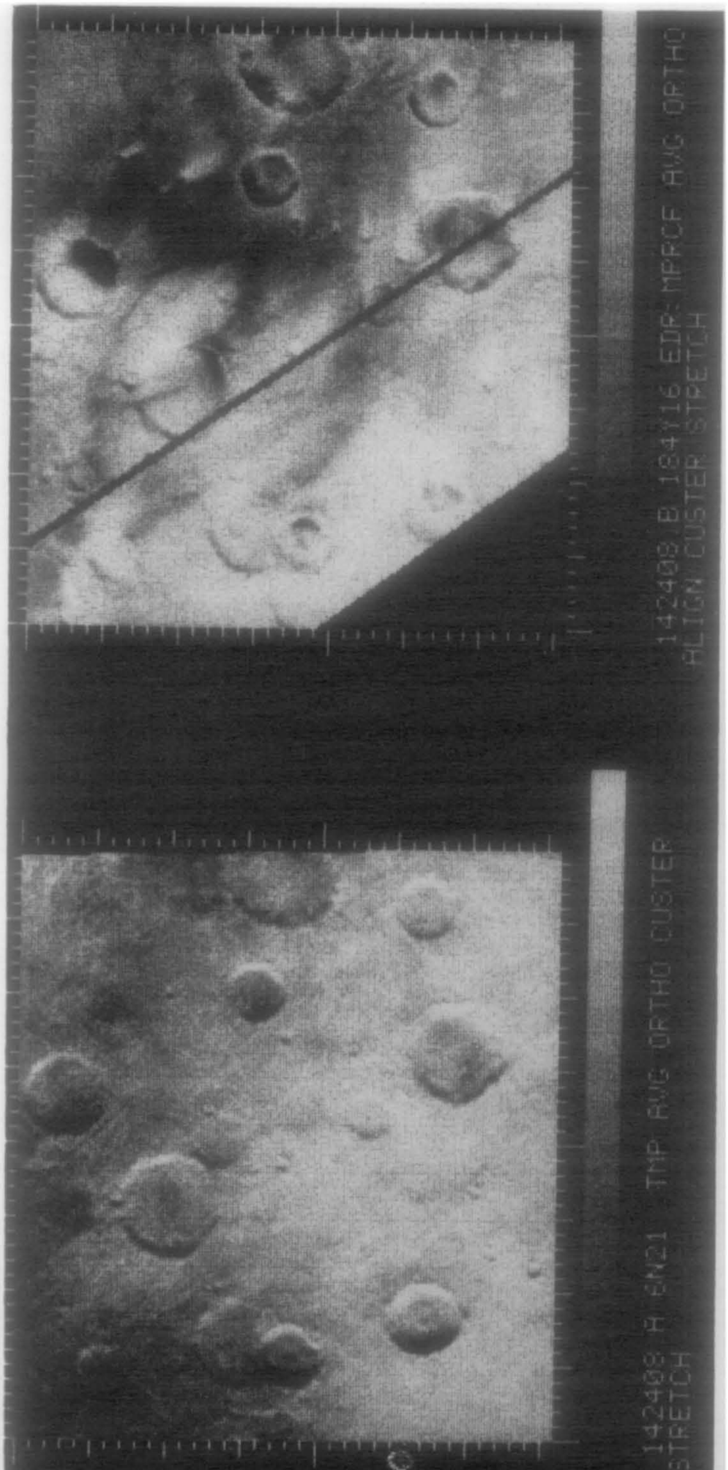

FIG. 22. Window C with R184/8189549. Contrast stretched. An important comparison showing the appearance, since 1969, of crater splotches and of diffuse dark albedo regions with superposed small white crater tails. ($K = 1.60$.)

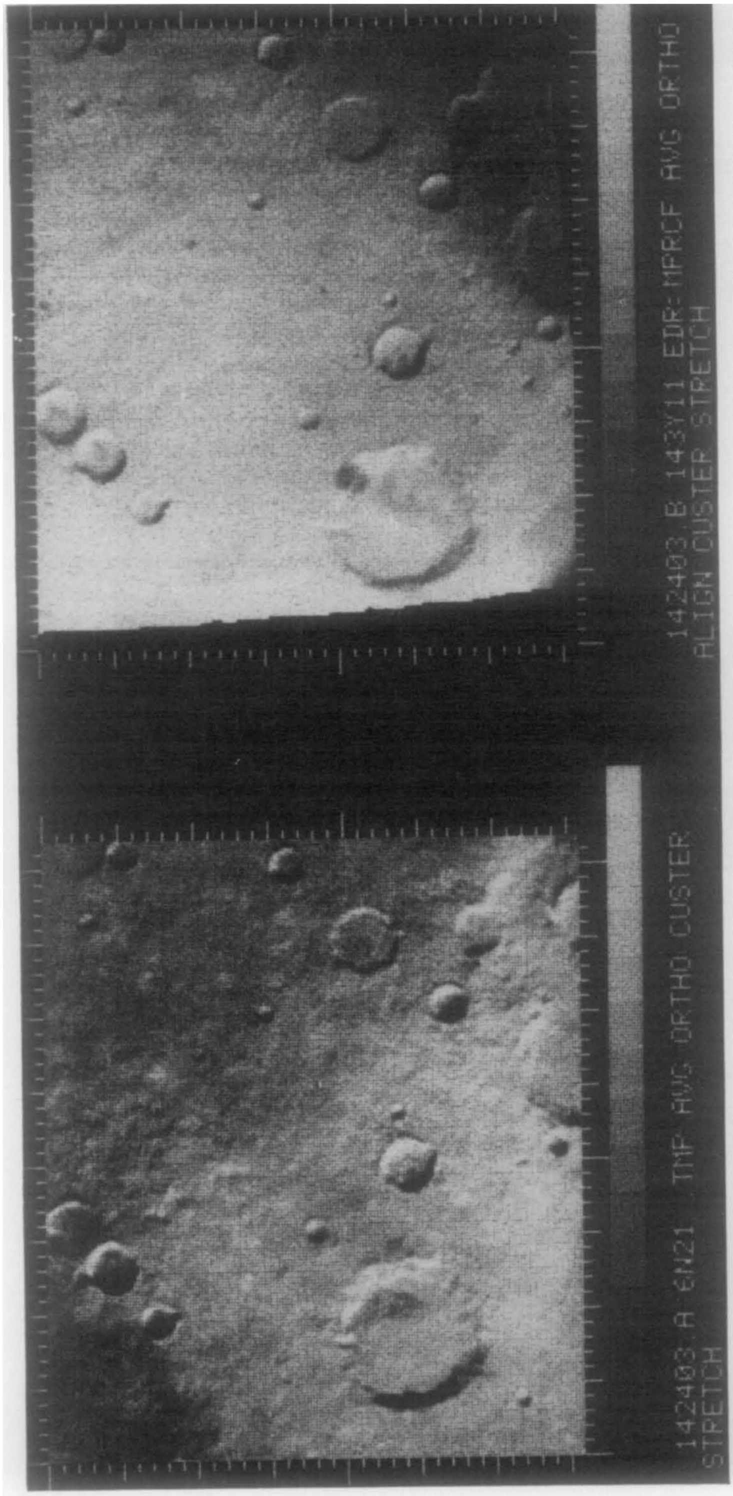

FIG. 23. Window D with R143/6714713. Contrast stretched. Little change has occurred in this window; a brightening may be indicated in the upper left corner, but this is photometrically uncertain since this area corresponds to a corner of the R143 frame. There may have been a relocation of the splotch in the larger crater at lower left. ($K = 1.50$.)

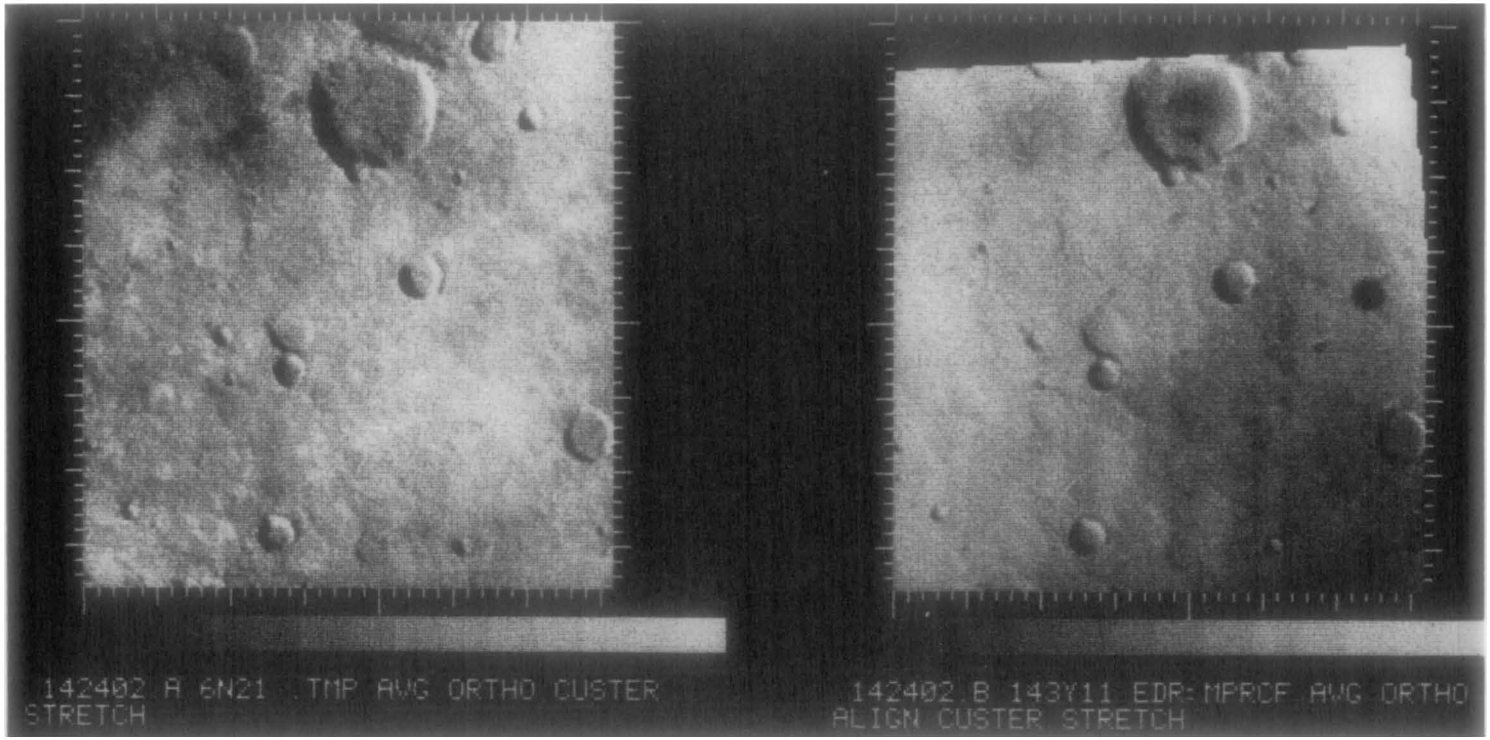

FIG. 24. Window E with R143/6714713. Contrast stretched. This provides an excellent example of a M6/M9 picture difference. No significant contrast changes are evident. The white streaky patchiness in this and other M6 frames is probably due to noise. The round dark spot near the right edge of the M9 window is a camera blemish. ($K = 1.50$.)

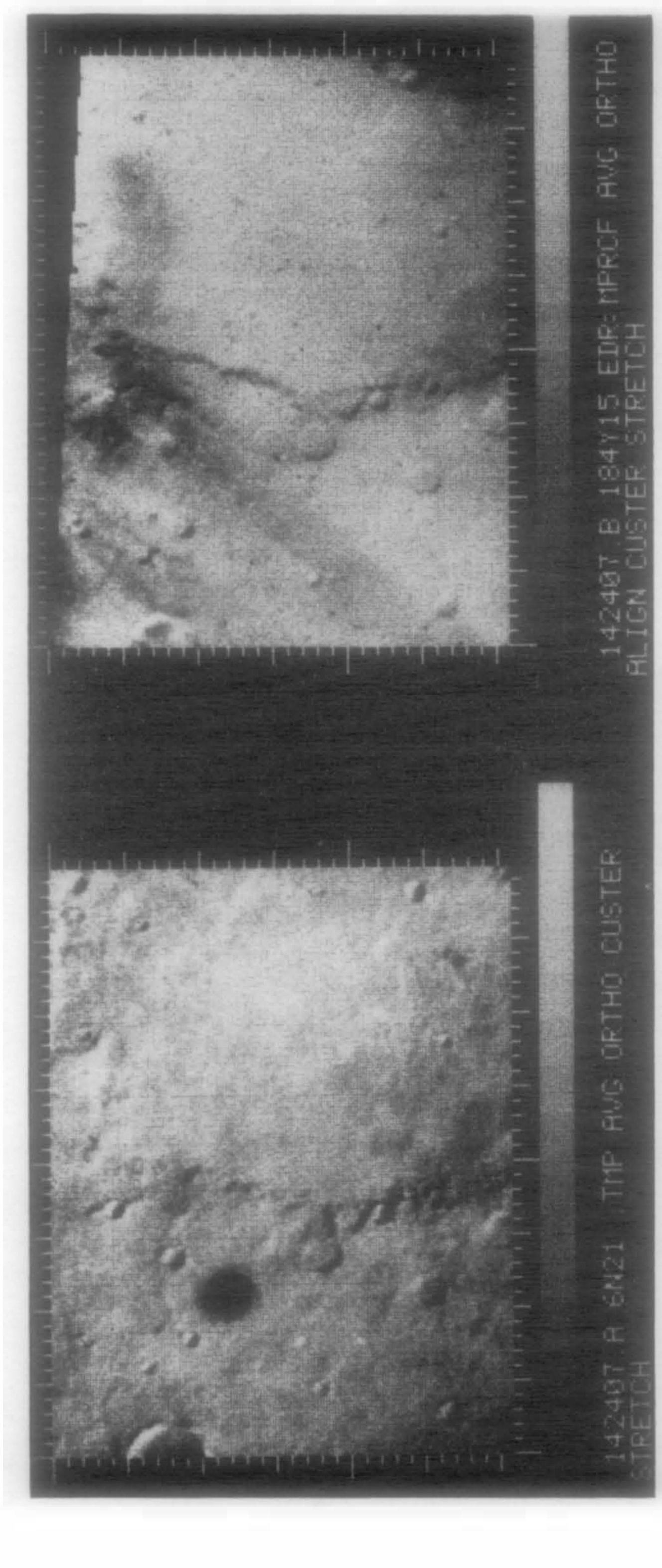

FIG. 25. Window F with R184/8189479. Contrast stretched. A bright and dark streakiness runs diagonally across the upper left corner of the M9 frame. Some of this appear to be due to diffuse bright crater tails trending up and to the right which are not evident in the M6 view. The intense dark spot in the M6 window is a camera blemish. ($K = 1.50$.)

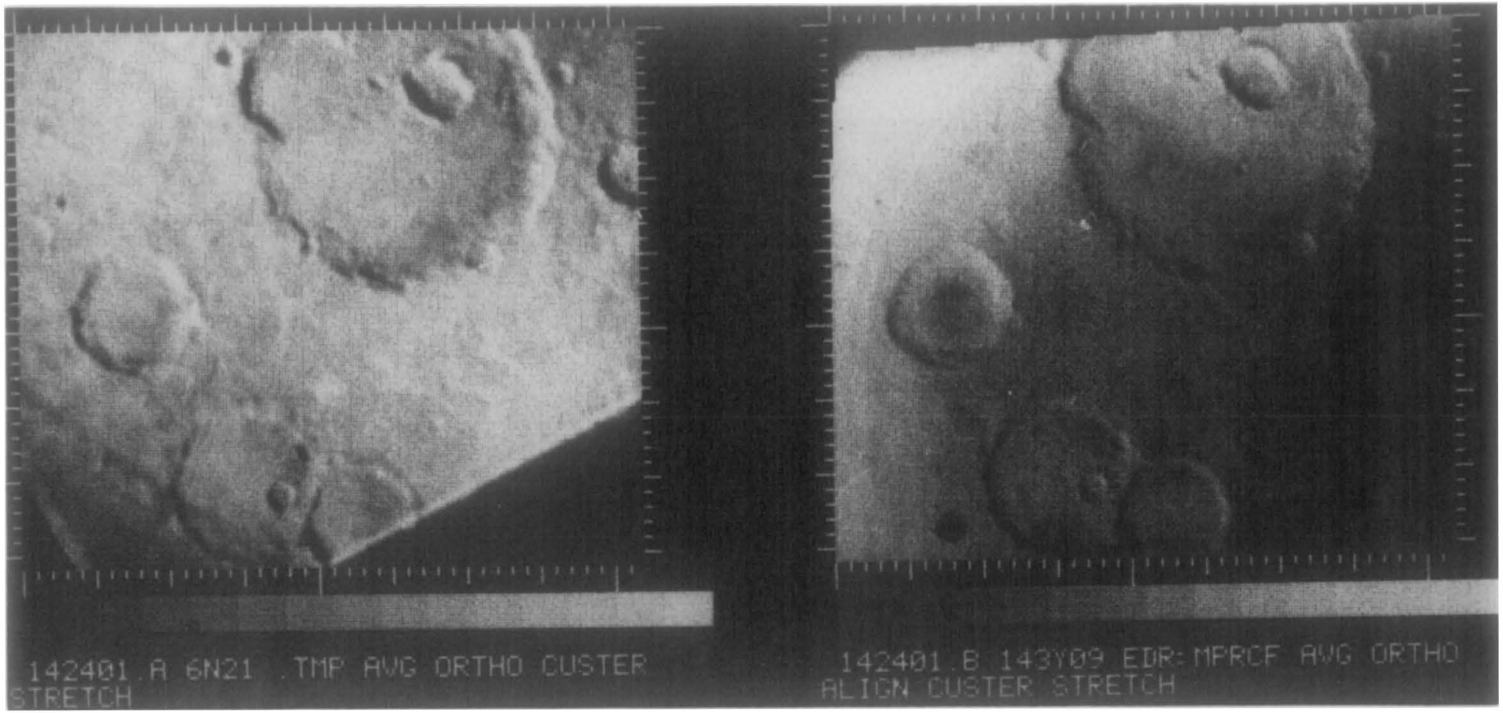

FIG. 26. Window G with R143/6714643. Contrast stretched. This comparison shows the possible appearance of a diffuse crater splotch at center left. The dark round spot in the lower left corner of the M9 window is a camera blemish. ($K = 1.65$.)

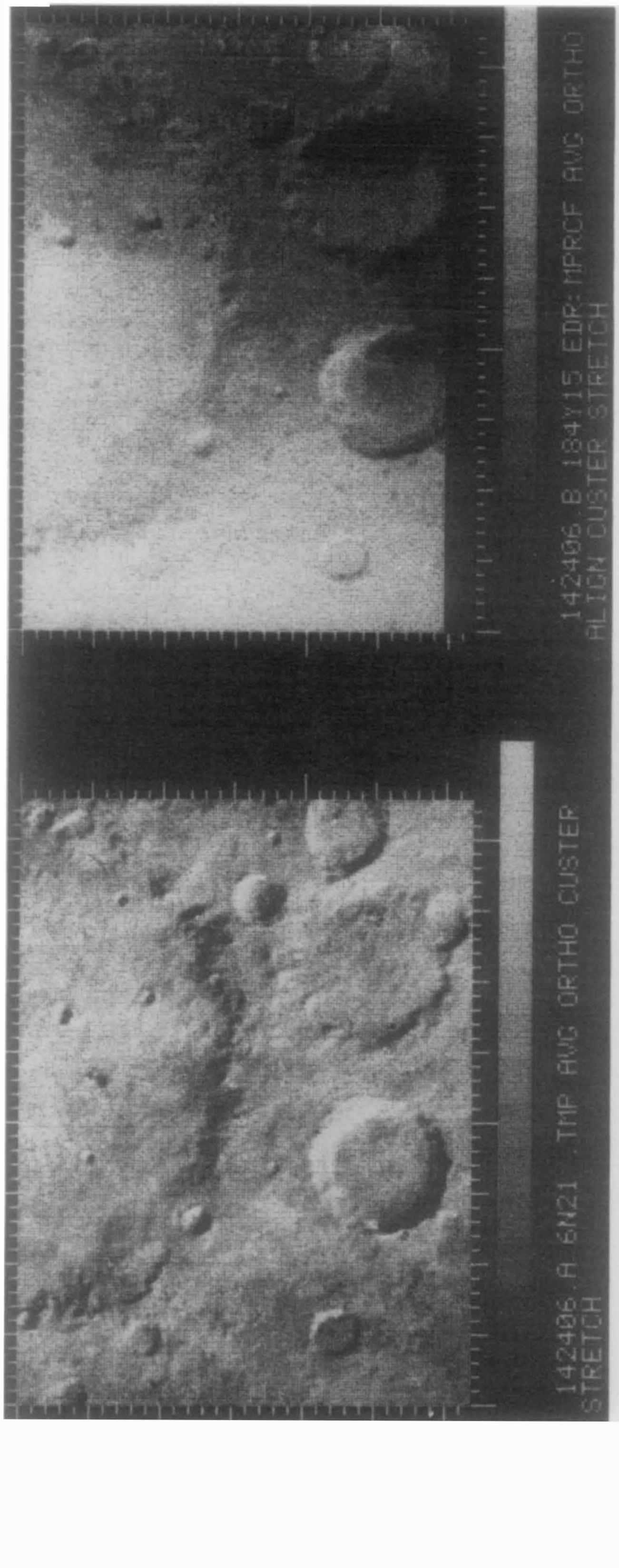

Fig. 27. Window H with R184/8189479. Contrast stretched. The appearance of dark albedo markings against the walls of the two craters at bottom is indicated in the M9 view. ($K = 1.50$.)

TABLE II

MARINER 7 A-FRAME DATA SELECTED FOR STUDY (COLLINS, 1971)

	Filter	Range (km)	Phase angle	Lighting angle	Viewing angle	Lat/long
7N11	G	6381	35°	52°	45°	57°S, 27°W
7N13	R	5886	35°	56°	43°	65°S, 17°W
7N23	G	4431	80°	33°	47°	34°S, 339°W
7N27	G	3656	80°	59°	24°	46°S, 308°W
7N29	R	3633	80°	71°	26°	41°S, 291°W

processing in detail. Some useful information can however be obtained. The non-frost covered area extends eastward of the Argyre basin, and shows several large craters (30°W, 50°S; 27°W, 48°S; 22°W, 45°S; and 17°W, 43°S). (Fig. 28). Mariner 9 frame Rev. 118/05812628 covers the region of these craters, but only a crude compari-

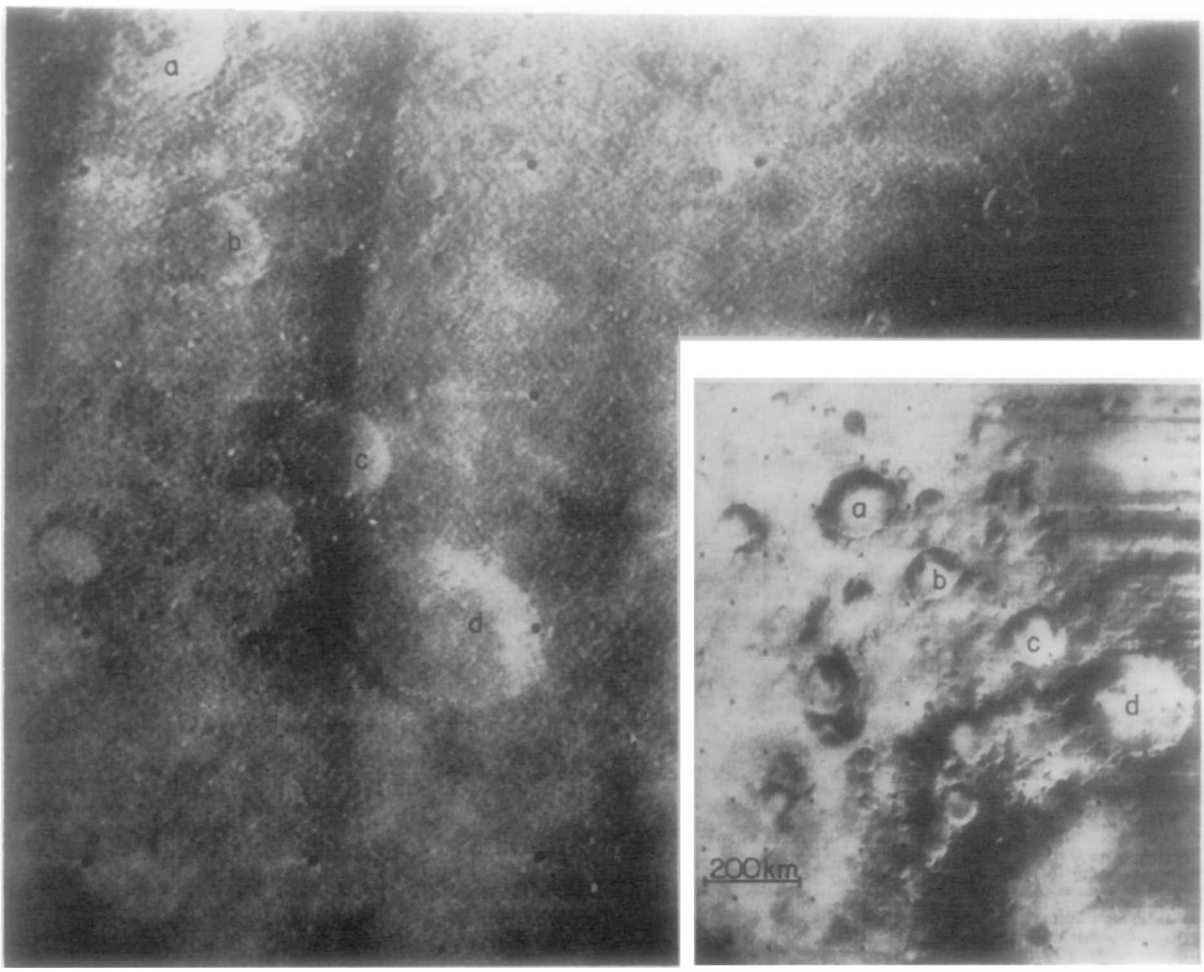

FIG. 28. The area of 7N11, compared with its appearance in M9 photographs (Rev. 118/05812628). A few of the corresponding features have been identified by letters.

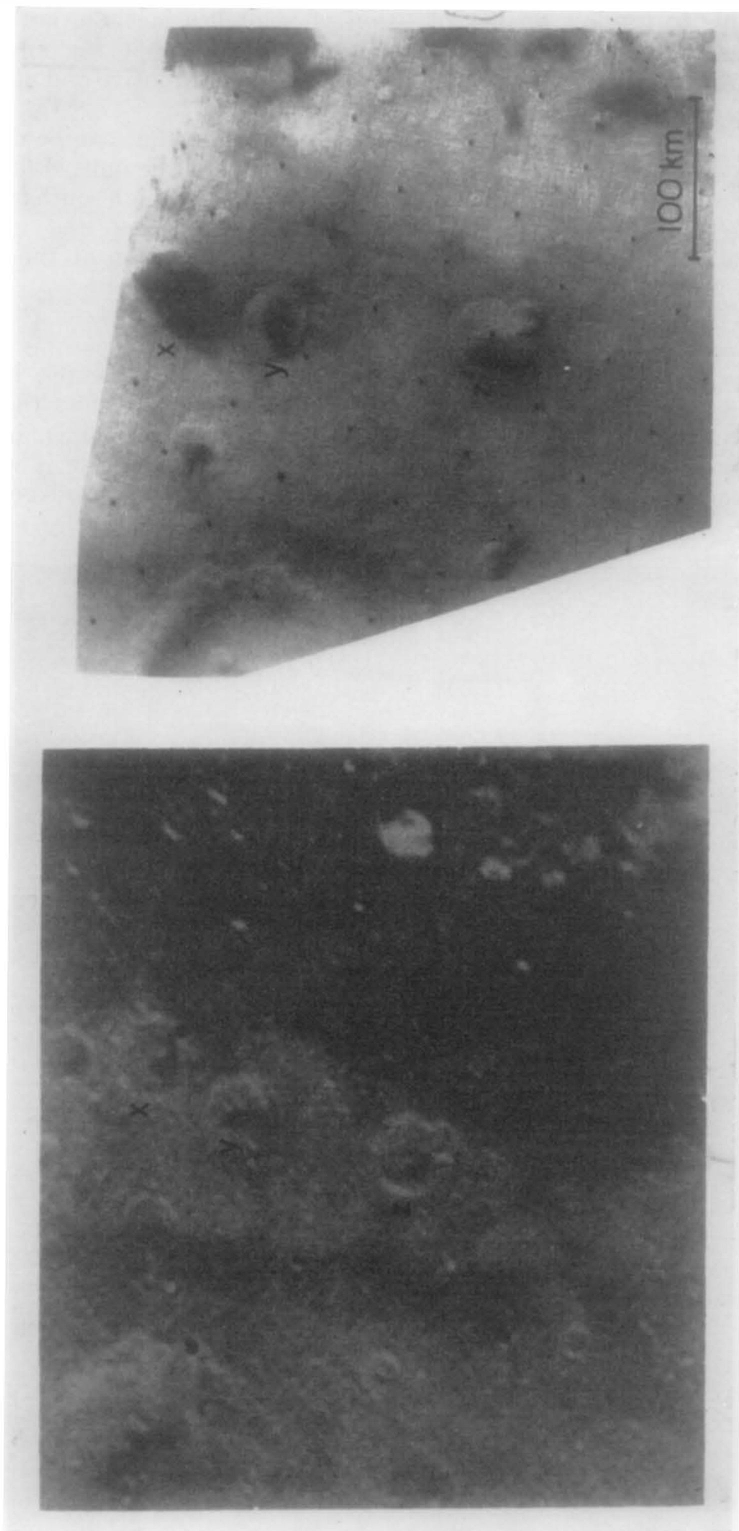

FIG. 29. The area of 7N13, compared with its appearance in M9 photographs (Rev. 106/05382688). Some of the corresponding features are identified by letters.

son is possible, due to the low quality of the M7 frame. The M9 frame seems to show a number of dark splotches which were probably not there in 1969.

B. 7N13

Part of this R frame shows the frost-free area near the cap's edge, in Noachis. The large crater in the upper left corner of the windows in Fig. 29 is located near 52°S, 10°W. Again this frame has severe residual image problems and cannot be processed in detail. The area of interest is covered by Mariner 9 frames Rev. 106/5382758 and Rev. 106/5382688. There are clear indications of dark splotches in these craters on the Mariner 9 photographs. Some indication of splotches in these craters is also present in 7N13, but the splotches are definitely more extensive and more streaky in the M9 frame.

The conclusion that can be drawn from 7N11 and 7N13—the only M 69 frames of frost free terrain at high southern latitudes —is that splotchiness was much more extensive in 1971 than at the Mariner 7 season in 1969.

C. 7N23

This Mariner 7 frame (G) has a very bland appearance. It shows the region of Mars around (340°W, 35°S), in Noachis. The entire right-hand side is washed out and suffers from residual image problems.

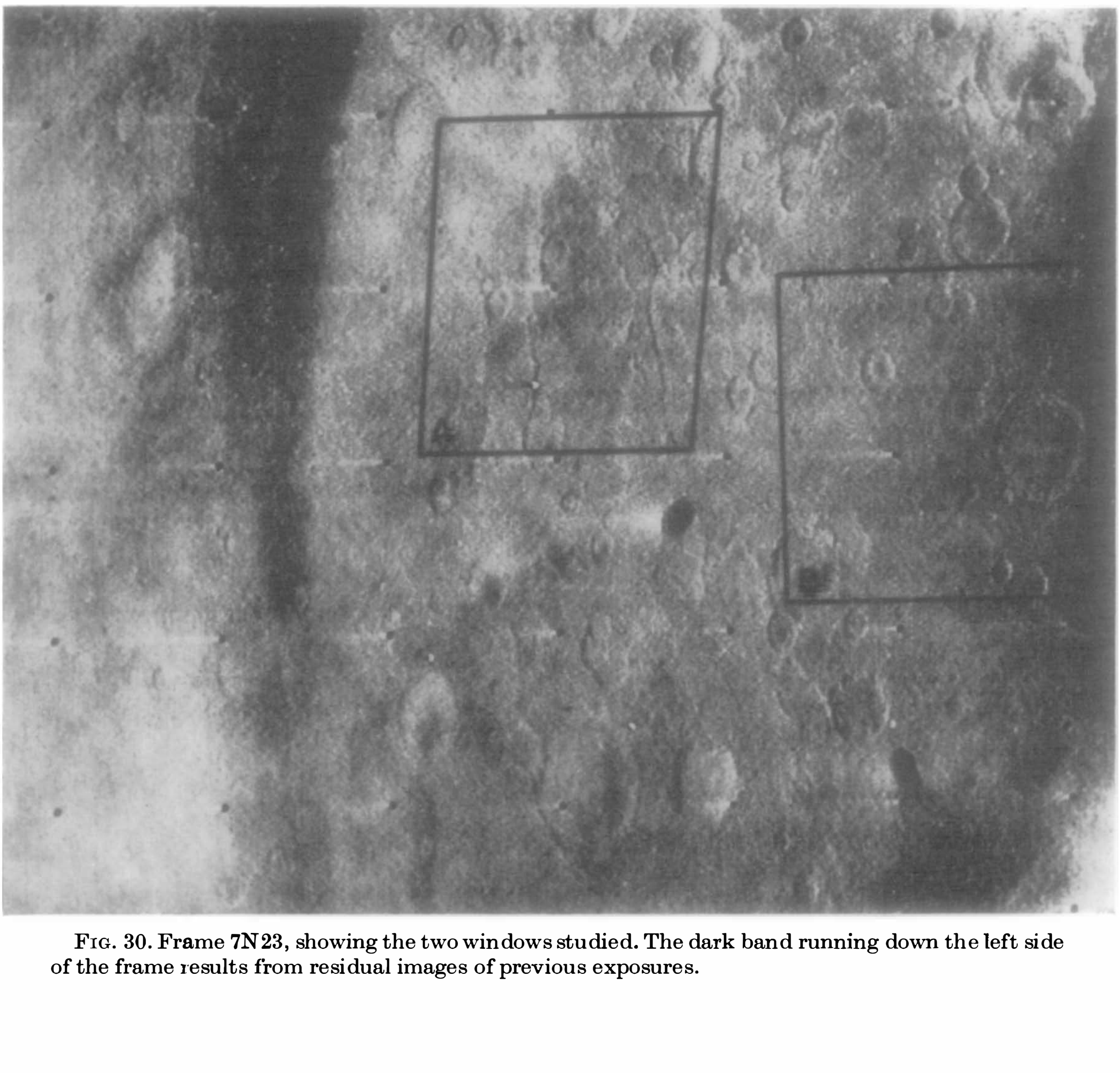

FIG. 30. Frame 7N23, showing the two windows studied. The dark band running down the left side of the frame results from residual images of previous exposures.

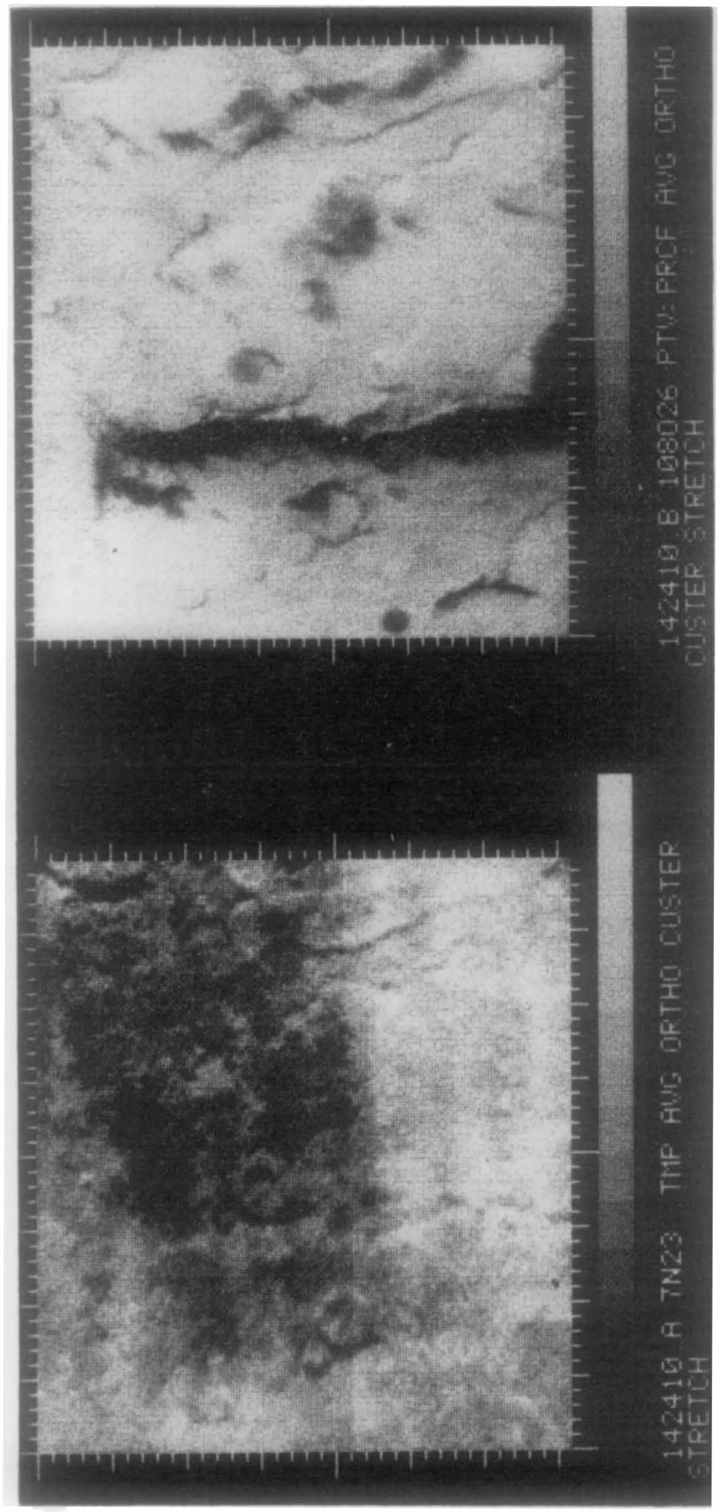

FIG. 31. Window A with R108/5455203. Contrast stretched. In spite of the low quality of **M7** picture data, the appearance of dark albedo material against a topographic barrier in the **M9** picture is evident. The vagueness of topographic detail in the **M9** window may be due to the possible presence of atmospheric dust. ($K = 1.90$.)

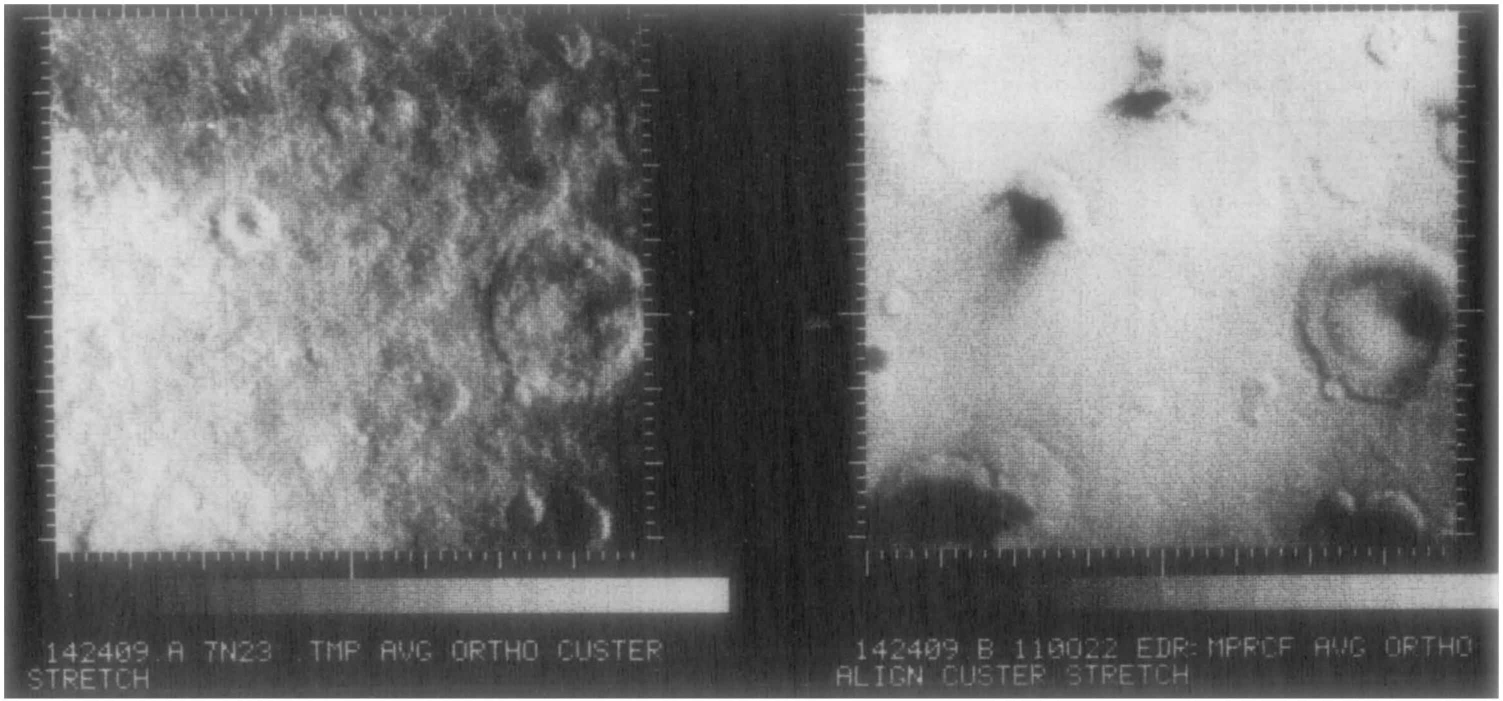

FIG. 32. Window B with R110/5527093. Contrast stretched. This comparison shows the appearance of several prominent crater tails in **1971**, and of very intense dark crater splotches (e.g., bottom left). Note especially the crater triplet at top center, with its prominent dark tail. This area was photographed at high resolution in **7N22** and can be compared with several **M9** B-frames. The comparison (Fig. 37) confirms that the dark tail was not present at the Mariner **7** season. ($K = 1.80$.)

The area is covered by M9 frames Rev. 110/5527028; 5527098; 5527168 and Rev. 108/5455208; 5455138; 5455068. A quick examination of these frames shows that in 1972 the area, far from being bland, was very splotchy.

Two windows (Fig. 30) in 7N23 were chosen for detailed study (Figs. 31, 32). Due to its rather poor quality this frame was not differenced extensively. Although a few craters had dark crater splotches at the Mariner 7 season (early spring) the degree of splotchiness both in and out of craters was considerably greater at the Mariner 9 season (late summer).

D. 7N27

This G-frame, centered near (310°W, 45°S), shows the boundary of Hellespontus and Hellas. The clearing of Hellas shown by this frame has already been discussed by Leovy *et al.* (1972).

This area is covered by Rev. 114/5671018; 5671088 and by Rev. 116/05743118. The M9 frames show much dark albedo material near the Hellas boundary and within some of the large craters. This material may have been there in 1969, although this is difficult to prove due to the poor photometric quality of 7N27. Whatever evidence for albedo changes there is in this frame supports the conclusion of increased splotchiness in 1971.

E. 7N29

This is an essentially featureless frame of Hellas. Although close to the terminator, it is probably featureless because Hellas was obscured at the time by dust ($L_s = 200°$), as it was during much of the Mariner 9 mission. Hellas finally began to clear near Rev. 237 ($L_s = 359°$) and was clear on Revs. 430/431 ($L_s = 44°$) (cf. Leovy *et al.*, 1972).

The main conclusions based on the study of the Mariner 7 near-encounter frames can be summarized as follows:

1. Judging from the region around Noachis (50°S, 10°W), although some dark splotches were present at the Mariner 7 season (early spring), the splotchiness was significantly more pronounced at the time of Mariner 9. Many of the dark splotches seen in this area on Mariner 9 photographs are definitely streaky. Such splotches are not evident on M7 photographs (7N11/13).

2. A significant increase in albedo contrast in Noachis and Hellespontus is revealed. The region was rather bland in 1969; there are numerous dark crater splotches, streaky splotches, and dark albedo markings along topographic barriers in the 1971 photographs (7N23/27).

3. A clearing in the Hellas basin occurred late in the Mariner 9 mission ($L_s \gtrsim 0°$). The floor of Hellas was obscured during southern spring (M7) and southern summer (M9).

4. Although 7N25 is a blue frame, some dark crater splotches are visible. This can be confirmed by comparing the overlap region of 7N23 and 7N25. A comparison of 7N25 with M9 photography indicates that many of the large crater splotches in Hellespontus have remained essentially unchanged in outline during the 2-yr interval betwen M7 and M9.

III. MARINER 6 and 7 B-FRAMES

Very few M 69 B-frames have M 71 B-frame overlaps. The search for such overlaps was facilitated by using the Stanford program NEWTRAN, which can be used to show the footprints of all B-frames in the vicinity of a particular frame. Figure 33 shows an example of a NEWTRAN output: the footprints of

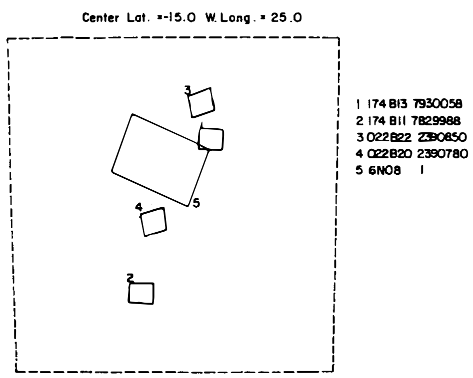

FIG. 33. NEWTRAN output showing M9 B-frame overlaps and near-overlaps with M6 B-frame 6N8.

M9 B-frames in the vicinity of 6N8. It is seen that only one Mariner 9 B-frame (R174: 7830024) marginally overlaps the area of 6N8. The footprint locations are based on two separate programs PEGASIS (M6 and 7) and POGASIS (M9). There is often a mismatch between the coordinate systems of the two programs, and such plots as that shown in Fig. 33 can only be used for guidance. In many cases the M 69 frames are of very poor quality, making a meaningful comparison with M9 data impossible.

Since the resolution of some Mariner 9 A-frames is only about four times less than that of typical M6 and M7 B-frames, useful information can be obtained by intercomparing some M6 and M7 B-frames with M 71 A-frames (see below).

The useful Mariner 6 frames include 6N6 to 6N22 (Table III). In the case of Mariner 7 the list consists of 7N6, 8, 22, 24, 26, 28 and 30) (Table III). Note that the polar M7 B-frames are not included in this study.

A. 6N6

This frame is best discussed in conjuction with 6N14 which it overlaps.

B. 6N8

This is a view of the partially collapsed terrain of Margaritifer Sinus. The small amount of overlap between this frame and Mariner 9 B-frame Rev. 174/7930068 is too marginal to be useful. The area is covered by Mariner 9 A-frame Rev. 174/7830024. The only possible change is the darkening (in the M9 frame) of a portion of the floor of the large crater seen in 6N8.

C. 6N10

This is a view of the cratered terrain in the bright region Aram which separates Margaritifer Sinus and Sabeus Sinus. Again, no Mariner 9 B-frame overlaps are available, but Mariner 9 A-frame Rev. 176/7902404 covers this area. The comparison is interesting in that a dark splotch in the largest crater in 6N10 is observed essentially unchanged in outline in the M9 frame.

D. 6N12

There are no Mariner 9 B-frame overlaps of this view of Sinus Sabeus, but Mariner 9 A-frame Rev. 139/06571358 covers this region. Since there is little on 6N12 which

TABLE III

MARINER 6 AND 7 B-FRAME DATA (COLLINS, 1971)

	Range (km)	Phase angle	Lighting angle	Viewing angle	Lat/long
6N6	5355	52°	17°	37°	10°S, 37°W
6N8	4778	52°	29°	25°	14°S, 26°W
6N10	4727	52°	46°	39°	1°S, 10°W
6N12	4428	52°	55°	38°	3°S, 0°W
6N14	4903	80°	19°	62°	13°S, 37°W
6N16	4105	80°	38°	42°	17°S, 18°W
6N18	3746	80°	52°	31°	16°S, 4°W
6N20	3546	80°	66°	21°	16°S, 351°W
6N22	3498	80°	76°	15°	15°S, 340°W
7N6	7552	44°	2°	46°	7°S, 359°W
7N8	6774	44°	10°	36°	17°S, 353°W
7N22	4818	80°	24°	56°	28°S, 346°W
7N24	4154	80°	41°	40°	38°S, 331°W
7N26	3778	80°	54°	29°	44°S, 316°W
7N28	3679	80°	66°	28°	41°S, 298°W
7N30	3636	80°	77°	27°	39°S, 284°W

is not evident as 6N13—an A-frame view taken with a red filter—the intercomparison of the areas is best done at A-frame resolution (Part I).

E. 6N14 (and 6N6)

These are overlapping B-frames of the chaotic terrain in Pyrrhae Regio. There are no Mariner 9 B-frame overlaps (after Rev. 100), although Mariner 9 A-frame Rev. 211/9161010 covers the area. No useful information about albedo variations is obtainable from the comparison.

F. 6N16

A view of the cratered region of Margaritifer Sinus. There are no useful Mariner 9 B-frame overlaps; the region is covered on Mariner 9 A-frame Rev. 176/7901914 (Fig. 34). A considerable increase in albedo contrast apparently occurred since 1969—including the appearance of dark crater splotches.

G. 6N18

A view of a large crater in Aram/Deucalionis Regio. There are no overlapping Mariner 9 B-frame (after Rev. 100). The area is covered by Mariner 9 A-frame Rev. 180/8045624, which indicates some slight splotch related albedo changes in the area since 1969. This impression is confirmed by an examination of 6N19.

H. 6N20

This B-frame view of the cratered terrain of Deucalionis Regio is covered by Mariner 9 A-frame Rev. 182/08117518. The region is marginally overlapped by two Mariner 9 B-frames Rev. 416/17/11443434 and

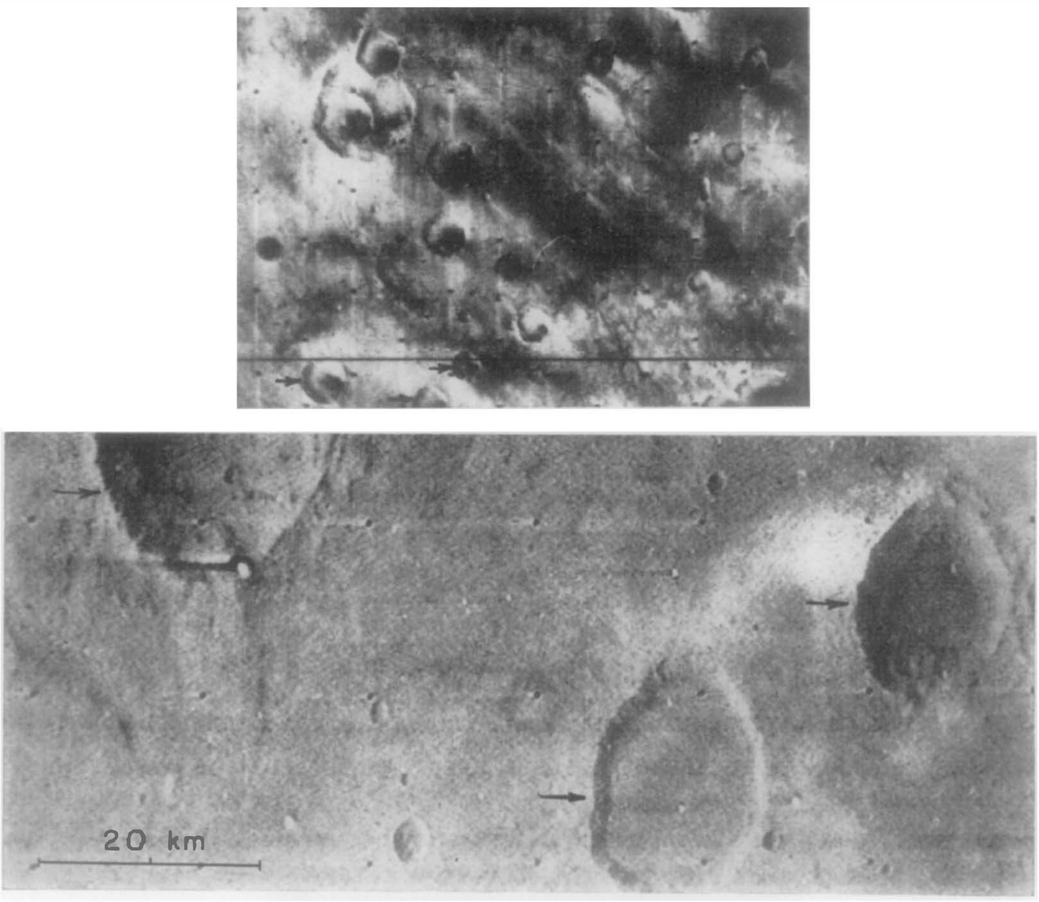

FIG. 34. Top: M9 A-frame Rev. 176/7901914. Bottom: A portion of M6 B-frame 6N16. Corresponding craters are indicated by arrows.

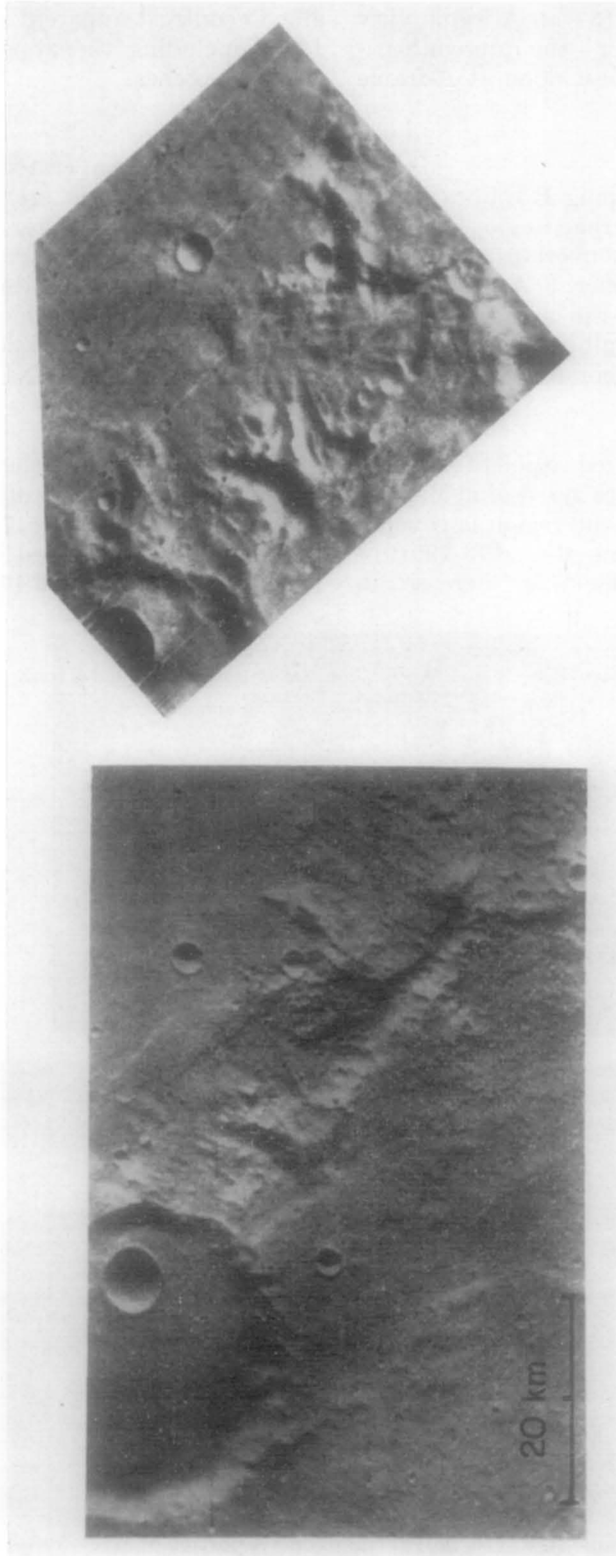

FIG. 35. Left: A portion of M6 B-frame 6N22. Right: M9 B-frame Rev. 223/9592454.

11443364. These frames cannot be usefully compared with 6N20. No changes are evident, and there are no strong albedo features in the area.

I. 6N22

Another view of the cratered terrain of Deucalionis Regio, overlapped substantially by Mariner 9 B-frame Rev. 223/9592425. There are no albedo features in the overlap area and no changes are evident (Fig. 35).

J. 7N6

This is a poor quality M7 frame of the cratered terrain in Meridiani Sinus. Adequate overlaps are provided by Mariner 9 A-frames (Rev. 180/8045768) and B-frames (Rev. 180/8045868; Rev. 533/13165358), but no useful conclusions can be drawn due to the poor quality of 7N6.

K. 7N8

No useful Mariner 9 B-frame overlaps exist. The area is covered by some A-frames, such as Rev. 182/8117518. At least one dark splotch is visible on the floor of the largest crater in 7N8, but it seems that most of the dark splotches

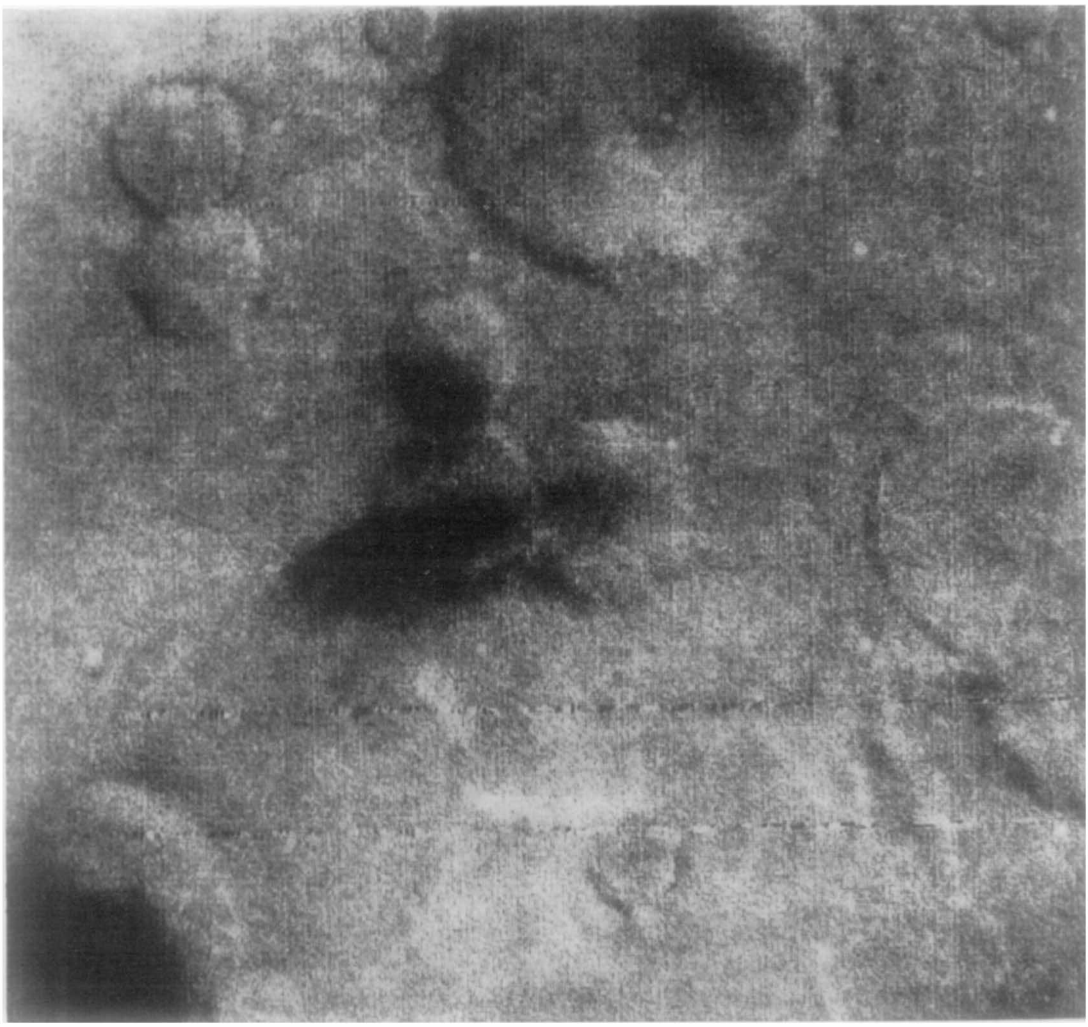

FIG. 36. Section of Mariner 9 A-frame Rev. 110/5527098 covering the region of M7 B-frame 7N24 shown in Fig. 37.

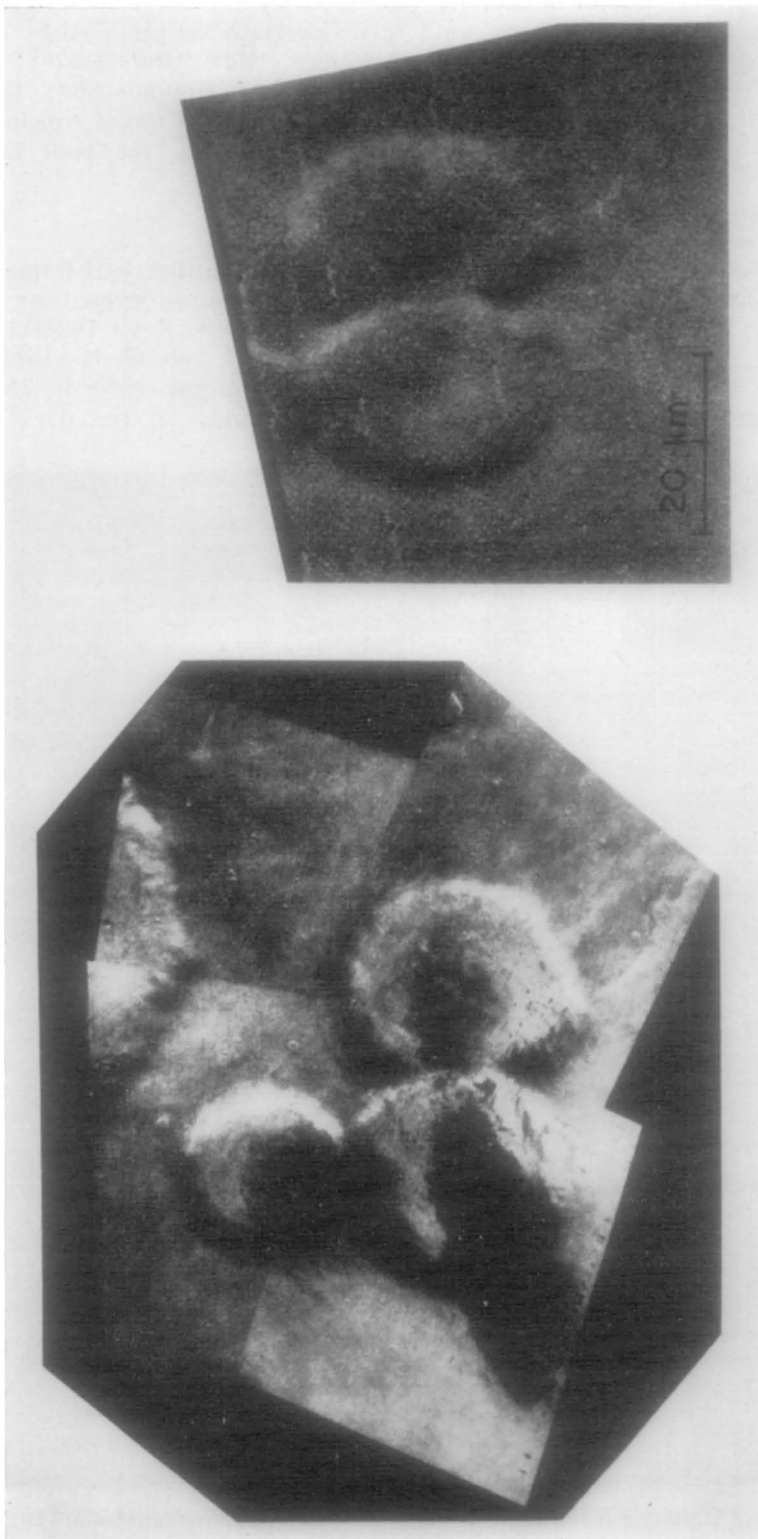

FIG. 37. Left: Mosaic of four M9 B-frames (Rev. 192/8476864-6934-6794-7004). Right: Same area as seen on M7 B-frame 7N24 (cf. Figs. 32 and 36.)

seen in the M9 pictures of this area were not present at the Mariner 7 season.

L. 7N22

This is a very oblique view of the cratered terrain in Pandorae Fretum. Two Mariner 9 B-frames which overlap this region are heavily obscured by dust (Rev. 118/5813918, 5813848), but the area is seen well on Mariner 9 A-frame Rev. 184/8189244. The comparison shows that at least one dark crater splotch in the overlap region seen in 1972 may not have been there in 1969. However, 7N22 is a poor quality frame.

M. 7N24

This frame of the cratered terrain in Noachis is covered both by Mariner 9 A-frames (Rev. 110/5527098) (Fig. 36) and B-frames (Rev. 192/8476864; 6934, 6794, 7004) (Fig. 37). It provides the best case for an intercomparison between M7 and M9 B-frames. Note the appearance of the prominent streaky dark splotch which is not evident in 7N24. The A-camera view of this region has also been compared with 7N23 (Fig. 32, top center). This confirms that this splotch was definitely not visible at the time of Mariner 7.

N. 7N26

This ridge area of Hellespontus is covered by Mariner 9 A-frames Rev. 114/5671088 and 5671168. There are no B-frame overlaps. No albedo markings are visible in the overlap region on either 7N26 or the Mariner 9 frames.

O. 7N28

This is a featureless B-frame of the floor of Hellas. A Mariner 9 B-frame which does not overlap but which is nearby (Rev. 118/5815178) is equally featureless.

P. 7N30

Another featureless B-frame of Hellas, taken very close to the terminator (i = 82°). A nearby Mariner 9 B-frame (Rev. 120/5887208) is also quite featureless.

Q. Conclusions

The main conclusion of Part II can be summarized as follows:

1. An increased splotchiness in the Deucalionis Regio, Noachis and Hellespontus regions at the M 71 season is indicated (7N8, 22, 24; 6N16, 18).
2. Some changes in splotch outlines and locations are evident (7N8).
3. A few dark crater splotches have remained unchanged in outline for at least 2yr (6N10).

IV: Discussion

The main conclusions of each section have already been summarized. The one striking trend is that the M9 images generally show considerably more contrast than the M6 and 7 views, despite the great sand and dust storm of the M9 mission, the initial effect of which should have been to decrease contrast.

In Meridiani Sinus the intercrater area is of a uniform tone (presumably dark) in the M6 picture (6N13), but is very patchy in the M9 photography. The same is true of many crater floors in the area. At the same time, large-scale changes in albedo boundaries have occurred. A similar pattern emerges from the study of 6N19 and 6N21 which cover the boundary of Deucalionis Regio and Meridiani Sinus. The M9 pictures show much more contrast with several splotches (both in and out of craters) evident in the M9 pictures, but absent in 6N19 and 6N21. There are, however, some crater splotches which can be identified in both sets of data, and whose outline has remained unchanged. They generally appear more contrasty in 1972 than at the M6 season.

In the 6N13, 19, and 21 regions, certain bright and dark streaks can be found in 1972 which were not present in 1969. This indicates that the time scale for the development of such streaks is <2yr. From M9 photography alone we know that the time scale for the development of many dark streaks is less than 20 days (Sagan *et al.*, 1972), but no bright streaks were observed to form during the entire

M9 mission. Of the 2000 or so bright streaks observed by M9 on Mars $\gg\sqrt{2000}$ have been carefully examined for such changes. In 6N13 there are both dark and bright streaks which can also be identified in M9 images—proving that the lifetime of such streaks can exceed 2 yr.

Figure 3 shows a significant extension of a dark crater splotch in 6N13 into a dark crater-associated streak in 1972. The predominant streak direction in 6N13 is the same as that in the M9 pictures of this region, indicating the same wind patterns at the two epochs.

The Mariner 7 pictures studied here cover the region of Noachis and Hellespontus. Again, the contrast seen in the M9 pictures is pronounced, whereas the M7 pictures are very bland. Numerous splotches in craters and associated with topographic features are seen in 1972. This is similar to the trend shown in the regions of 6N13, 6N19 and 6N21 (above). This trend towards increased contrast and splotchiness in 1972 is confirmed by the limited study of B-frames possible with so few overlaps (Part III). These frames indicate that there are a few splotches which have not changed in location between M6 and M9, although their contrast is much higher in 1972. Generally, however, there are many more splotches in 1972. It cannot be that the M6 B-camera is to blame, although it did exhibit low intrinsic contrast—as the high contrasts seen in the far encounter frames demonstrate.

We have previously noted (Sagan *et al.*, 1973) that large dark particles (of the order of 200 μm radius) are more easily moved directly by Martian winds than small bright particles (several tens of μm radius). The finding of the present paper, that brightening events occurred between 1969 and 1972, may be interpreted as a particle size related effect. The two sets of data are separated by the great sand and dust storm of 1971 which by all accounts represents one of the most severe such storms on record. The picture which emerges is of a Mars where the winds are often adequate to move dark material but where unusual meteorological events are required to move significant quantities of bright material over large distances. We stress again (cf. Sagan *et al.*, 1973) that dark saltating particles eject bright smaller particles into the atmosphere by momentum exchange at the surface, and that this is probably the primary cause of motion of small particles except during a major storm. This interpretation is consistent with the observed greater prominence of crater streaks—especially bright crater streaks—in Mariner 9 than in Mariner 6 data. These more pronounced crater streaks and sharper albedo boundaries may be a consequence of unusually high winds in the 1971 global storm. Future orbital missions to Mars may help determine the lifetime of bright streaks (which may well be positionally-variable on Mars), thus allowing an estimate of the frequency of anomalously high winds necessary for the production of bright streaks.

The study of visibility in Hellas between the M 69 and M 71 missions clearly shows that variations in the visibility of surface features is positionally dependent. The absence of detail in Hellas as observed by Mariner 69 was first interpreted (Sharp *et al.*, 1971) in terms of special erosional agents unique to Hellas. However Sagan, Veverka, and Gierasch (1971) proposed that the very high-speed slope winds generally expected to be running around the interior walls of Hellas can produce a semi-permanent dust haze above this region, obscuring surface detail. This latter view seems to be confirmed by the partial emergence of detail in Hellas later in the Mariner 9 mission as discussed above. Re-examination of the Mariner 1969 observations of Hellas (Leovy *et al.*, 1972) shows that some detail on the floor of Hellas may have been visible even in 1969.

The above and other regularities found from the comparison of M 69 and M 71 photography can be understood on the following model, which we offer as adequate to explain many of the observables but not as necessarily unique: Near perihelion each Martian year, a global sand and dust storm develops. Its severity varies from opposition to opposition. The storm lifts fine bright sand and dust high into the atmosphere. Larger darker particles fall out rapidly and are therefore transported only relatively short distances laterally. Smaller brighter particles require much longer times to fall out according to the Stokes-Cunningham equation and are therefore capable of covering dark material at great distances from their sources. One consequence of global dust storms will therefore be a brightening of terrains. Locales which for reason of topography or local roughness are not well covered by the dust fallout, or which are rapidly swept clean of fine dust by winds, will emerge as areas of high relative contrast. According to this scheme, Mariner 9 photography shows considerably more contrast than Mariner 6 and 7 photography because many areas are still covered with relatively bright dust. Eventually winds will sweep the fine dust, lifted by momentum exchange with larger particles, into microtraps, so that half a Martian year later (at the Mariner 6 and 7 season) the contrast in such areas as Meridiani Sinus will be low because little bright dust covering remains. The term "microtrap" is meant to include all crevices between rocks, pebbles and large particles into which smaller particles can be swept and become shielded from ambient winds. We stress that the bright dust described in the preceding few sentences is bright only relative to the surrounding dark terrain; it may well be "dark" relative to the multiple scattering albedo of a yellow cloud or to the top of the Martian dust storm at its maximum activity.

Global brightening requires in this scheme anomalously high winds; a progressive decline in contrast requires more generally available winds.

Areas which appear dark relative to surrounding terrain in Mariner 9 photography may be either those which were inefficiently covered by fine bright dust or those which are preferentially scoured of fine bright dust by winds. Preferential deposition and preferential deflation are both topographically controlled.

This comparison of Mariners 6 and 7 with Mariner 9 photography of Mars suggests that important new information about Martian seasonal and secular changes, dust storms, and local meteorology can be derived from a future orbital photography mission. Acquiring the full range of areocentric longitudes as well as a very long time baseline are equally important. For example, surface brightening events may be ready indicators of the times and places of the highest winds on Mars. For the generation of sand and dust storms and for eolian erosion (Sagan, 1973) the highest winds, even if very infrequent, may be of the greatest interest. The Viking 1976 orbiters can play a major role in extending such studies. But the ideal instrument is a long-lived orbital camera system with an absolute photometric accuracy of better than a few percent.

Acknowledgments

This work was supported by NASA Grant NGR 33-010-220. We are grateful to J. Lederberg, E. Levinthal and P. Fox, and thank the staff of the Image Processing Laboratory at JPL, for producing the mosaic shown in Fig. 37. Constructive discussions of an earlier draft were supplied by R. Arvidson and B. A. Smith.

References

Antoniadi, E. M. (1930). "La Planete Mars." Hermann, Paris.

Collins, S. A. (1971). The Mariner 6 and 7 pictures of Mars. NASA SP-263, Washington, D.C.

Danielson, G. E., Jr, and Montogomery, D. R. (1971). Calibration of the Mariner Mars 1969 television cameras. *J. Geophys. Res.* **76**, 418–431.

Leovy, C., Briggs, G., Young, A. T., Smith, B. A., Pollack, J., Shipley, E., and Wildey, R. (1972). Mariner 9 television experiment: Progress report on studies of the Mars atmosphere. *Icarus* **17**, 373–393.

Levinthal, E. C., Green, W. B., Cutts, J. A., Jahelka, E. D., Johansen, R. A., Sander, M. J., Seidman, J. B., Young, A. T., and Soderblom, L. A. (1973). Mariner 9—Image processing and products. *Icarus* **18**, 75–101.

SAGAN, C., VEVERKA, J., AND GIERASCH, P. (1971). Observational consequences of Martian wind regimes. *Icarus* **15**, 253.

SAGAN, C., VEVERKA, J., FOX, P., DUBISCH, R., LEDERBERG, J., LEVINTHAL, E., QUAM, L., TUCKER, R., POLLACK, J. B., AND SMITH, B. A. (1972). Variable features on Mars: Preliminary Mariner 9 results. *Icarus* **17**, 346–372.

SAGAN, C., VEVERKA, J., FOX, P., DUBISCH, R., FRENCH, R., GIERASCH, P., QUAM, L., LEDERBERG, J., LEVINTHAL, E., TUCKER, R., EROSS, B., AND POLLACK, J. B. (1973). Variable features on Mars. 2. Mariner 9 global results. *J. Geophys. Res.* **78**, 4163–4196.

SHARP, R. B., SODERBLOM, L. A., MURRAY, B. C., AND CUTTS, J. A. (1971). The surface of Mars. 2. Uncratered terrain. *J. Geophys. Res.* **76**, 331–342.

SLIPHER, E. C. (1962). Mars. Lowell Observatory, Flagstaff, Arizona.